

4.6 THE SODIUM-POTASSIUM PUMP AND $\text{Na}^+\text{-K}^+\text{-ATP-ASE}$

Ion pumps maintain the active transport system. Most animal cells maintain a higher concentration of K^+ ion inside the cell while a higher concentration of Na^+ ion outside the cell is required. The actual concentration of the ions differs for different types of cells. For a typical cell, the concentration ratios are : $[\text{Na}^+]_{\text{outside}}/[\text{Na}^+]_{\text{inside}} \approx 15$, $[\text{K}^+]_{\text{inside}}/[\text{K}^+]_{\text{outside}} \approx 25$. The high concentration of K^+ ion inside the cell is required for some vital processes occurring within the cells. K^+ ion is required for *glucose metabolism, protein biosynthesis, and activation of some enzymes (e.g. pyruvate kinase)*.

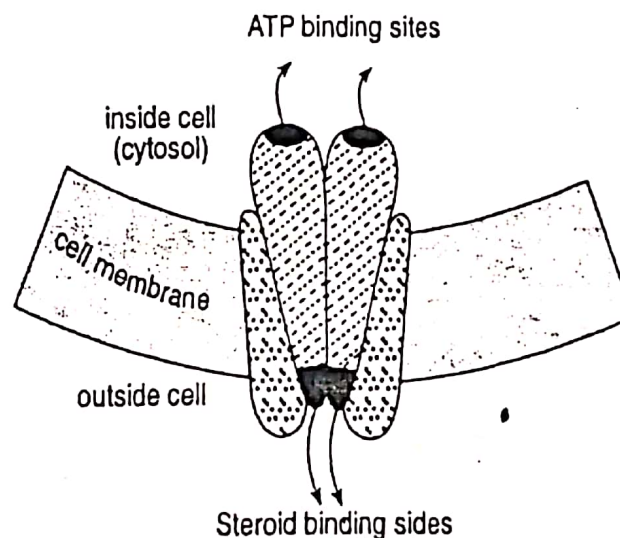


Figure 4.6.1: Schematic representation of the subunits ($\alpha_2\beta_2$) of $\text{Na}^+\text{-K}^+\text{-ATP-ase}$.

The concentration gradients for Na^+ and K^+ ions are maintained by the $\text{Na}^+\text{-K}^+$ pump driven by an integral enzyme, known as $\text{Na}^+\text{-K}^+\text{-ATP-ase}$ (Mol. Wt. ≈ 280 kDa). Energy is obtained from the hydrolysis of ATP to run the active transport process. The enzyme ($\alpha_2\beta_2$ tetramer) contains two α -subunits (Mol. Wt. ≈ 100 kDa for each subunit) and two β -subunits (Mol. Wt. ≈ 40 kDa for each subunit) (cf. Fig. 4.6.1). The larger unit (i.e. α_2) contains the ATP binding site. The ATP binding

sites are at the one end of the α -chains (in the cytosol side) while at the other end (in the outside) the steroid inhibitor binding sites are present. In the function of the pump, this α_2 unit actually acts as the revolving door. The α -chains contain the selective metal binding sites and phosphorylation sites. The α -chains traverse the plasma membrane. The β -chains mainly contain the carbohydrate.

To run the pump, Mg^{2+} plays a crucial role in two ways : **catalysis in ATP hydrolysis and structure-forming effect** to change the protein conformation. In the function of the Na^+-K^+ -pump, one cycle involves the transport of $3Na^+$ ions from inside the cell to outside the cell and $2K^+$ ions from outside the cell to inside the cell. Binding of three Na^+ ions with the protein (α_2 unit) changes the local polarities so that it is favourable to bind an ATP molecule which is hydrolysed by ATP-ase. This hydrolysis is catalysed by Mg^{2+} . During the hydrolysis, the α_2 -unit is phosphorylated at the aspartate site and ADP is released. This phosphorylation changes the conformation of the protein. For this conformation change, presumably Mg^{2+} plays an important role as Mg^{2+} is known to have a **strong structure-forming property**. This conformational change is called *eversion*, whose function can be compared with the motion of a revolving door. In this new conformation, the Na-binding sites become open to outside and the binding sites cannot bind Na^+ ions as strongly as before. This leads to the release of Na^+ ions to the extracellular fluid. Then the open channel binds $2K^+$ ions from outside and this binding causes dephosphorylation from the protein chain. This dephosphorylation causes an *eversion* which opens the K^+ -binding sites open to cytosol (inside the cell). In this conformation, K^+ is not bound as strongly as before and K^+ ions are released into the cytosol. This leads to the original conformation ready to take up the Na^+ ions to initiate a new cycle. The overall process is schematically shown in Fig. 4.6.2

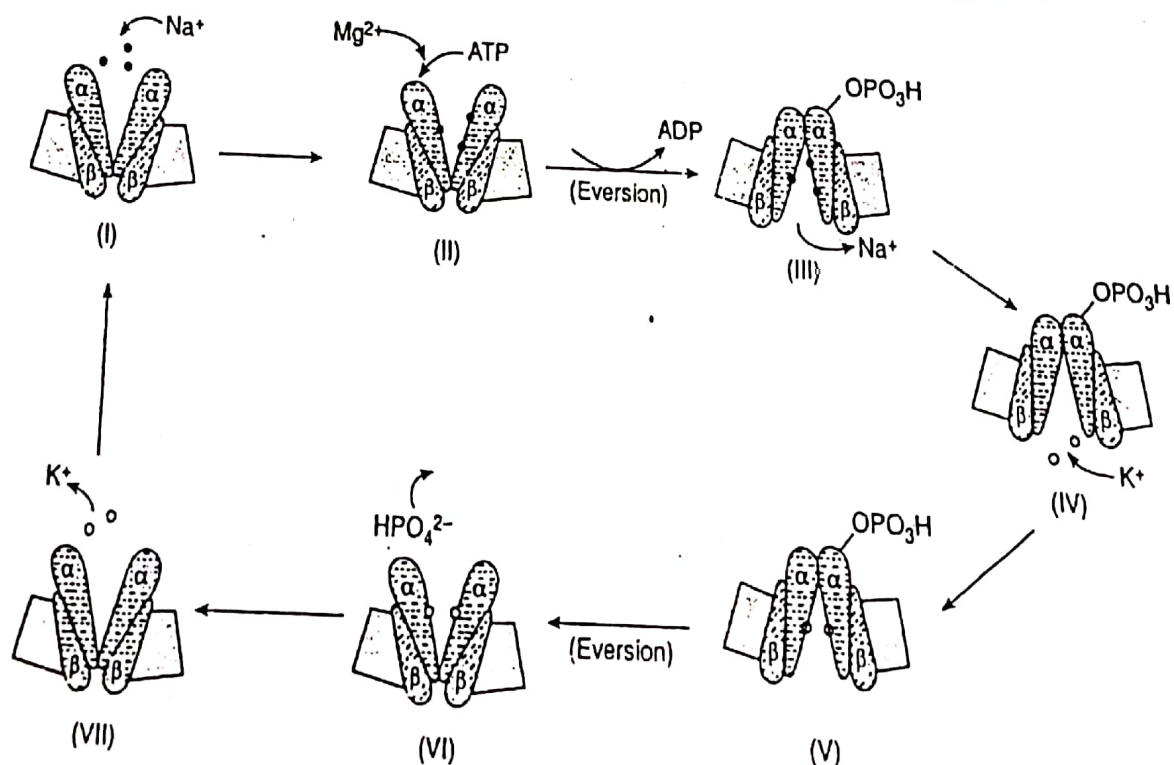
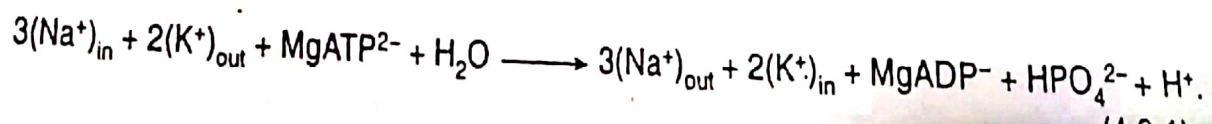


Figure 4.6.2 : Schematic representation of the functioning of Na^+-K^+ -pump.

The overall process is :



In the protein ($\alpha_2\beta_2$), the two α -subunits actively participate in binding Na^+ , K^+ and phosphorylation, while the β -subunits work in corporation. The metal binding sites are not yet fully characterised. It is suggested that for binding Na^+ , the α -subunits probably offer 6 hard O sites while for binding K^+ , 7O sites or 7O and 1N sites are involved.

The whole transport model can be explained by two different conformations E_1 and E_2 which can be mutually converted through **eversion**. The E_1 -conformation projects the ion binding sites towards the cytosol site, while the E_2 -conformation projects the ion binding sites outside the cell. The E_1 -conformation is selective for Na^+ ion while the E_2 -conformation is selective for K^+ ion. In the E_1 -conformation, Na^+ -binding triggers phosphorylation while in the E_2 -conformation K^+ -binding triggers dephosphorylation. The E_2 -form is stabilised by phosphorylation while the E_1 -form is stabilised by dephosphorylation. The process is schemetically shown in Fig. 4.6.3.

It is noted that vanadate (VO_4^{3-}) even at extremely low concentration can inhibit the function of Na^+-K^+ -pump. The VO_4^{3-} and PO_4^{3-} moieties are structurally similar and VO_4^{3-} can compete with PO_4^{3-} . Removal of PO_4^{3-} through hydrolysis can occur easily and in fact this dephosphorylation (from an aspartate moiety) causes an eversion to change the conformation. But if vanadate is bound with the aspartate moiety, then its removal through hydrolysis cannot occur to carry out the eversion, and consequently the bound K^+ cannot be released.

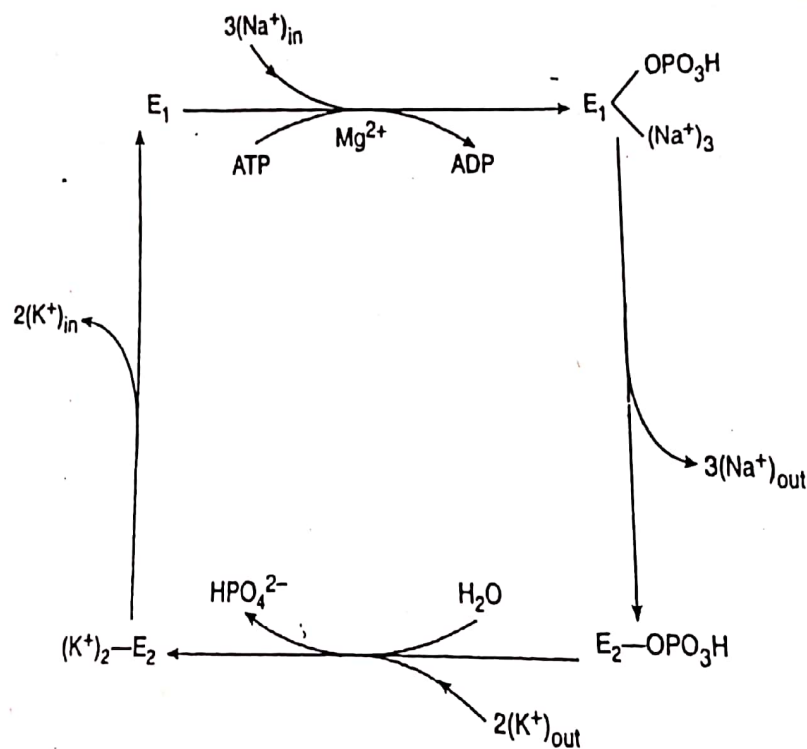


Figure 4.6.3: Schematic representation of the functioning of Na^+-K^+ -pump in terms of two different conformations (E_1 and E_2).

Selectivity of the Na^+-K^+ -pump : From the proposed mechanism, it is evident that the eversion changes the selectivity of the system towards Na^+ and K^+ . In one conformation (E_1) it is selective towards Na^+ while in another conformation (E_2), it is selective towards K^+ . Both Na^+ and K^+ ions are hard cations and they are not good complex forming centres. But Na^+ is harder and its complexing power is greater compared to that of K^+ . This is mainly due to the smaller size of Na^+ (cf. $r_+ = 133$ pm for K^+ and $r_+ = 95$ pm for Na^+). In fact, Na^+ is more strongly hydrated than K^+ as

evident from their hydration energy (cf. -302 kJ mol^{-1} for Na^+ , and -230 kJ mol^{-1} for K^+). Thus the bases stronger than H_2O will bind Na^+ preferably while the bases slightly weaker than H_2O can also displace K^+ from its hydration sphere. This small enthalpic disfavour (i.e. $\Delta H = +ve$) in binding K^+ in a macrocyclic cavity is compensated by the entropic favour (cf. $\Delta G = \Delta H - T\Delta S$, $\Delta S = +ve$; **macrocyclic effect**; cf. Sec. 1.5, 4.3, 4.4.3). In the case of Na^+ binding, the basicity of the ligating sites should be better (or at least comparable) than water otherwise ΔH will be highly positive (mainly due to high dehydration energy of Na(aq)^+) and this too high enthalpic disfavour cannot be compensated through complexation by a macrocycle. At the same time, the preference is also decided by the required metal-ligand distance (which is required to be longer for K^+). Definitely, the macrocyclic cavity size to bind K^+ must be larger than that required to bind Na^+ .

The actual binding sites to cause this selectivity are not known. Probably, the pump uses crown ether or cryptand or other related ionophores whose ligand basicity and cavity size may simultaneously work to cause the selectivity. In fact, for K^+ , a larger ring size with the relatively less hard binding sites will be more suitable while for Na^+ , a relatively smaller ring with the harder binding sites will be more suitable.

5.3 BIOLOGICAL OXYGEN CARRIERS

Small organisms require no oxygen carrier beyond simple diffusion. Some worms use **nonheme iron proteins** called **hemerythrin (Hr)** for this purpose. Lobsters, crabs use a copper containing protein called **hemocyanin (Hc)** for oxygen transport. In higher animals like mammals, oxygen transport and its storage are conducted by two **heme proteins** **hemoglobin (Hb)** and **myoglobin (Mb)** respectively. The dioxygen storage proteins are generally prefixed **myo** (from Greek root **mys** meaning muscle). Thus the word **myoglobin** originates. For **hemerythrins**, there also exists a chemically similar dioxygen storage protein described as **myohemerythrin**. Some organisms use **hemocyanin** for dioxygen transportation and use **myoglobin** for dioxygen storage. Hb and Mb constitute the red matter of our blood. 100 ml of normal body blood at body temperature can dissolve 20 ml of O_2 (at 760 Torr) while 100 ml of blood plasma (without any Hb and Mb) can absorb only 0.3 ml O_2 under identical conditions. These two proteins, Hb and Mb also play important roles in CO_2 transport from working tissues to lungs and in acid-base balance of blood. Depending on the nature of living species, hemoglobins differ **structurally**. In vertebrates, Hb is tetrameric (e.g. Hb-A in human), in some invertebrates Hb may contain as many as 192 subunits and these high-molecular-weight Hbs of arthropoda are referred to as **erythrocrucorin (Er)**. In some annelid worms, **Fe(II)-protoporphyrin-IX (i.e. heme b)** unit is replaced by **chloroheme unit** (having different substitutions on the porphyrin ring, cf. Fig. 7.5.1.1) to give **chlorocruorin (Ch)** which becomes green (Greek word **chloros** means green) on oxygenation. Ch also consists of 192 subunits. Vanadium in the form of **hemovanadin** is probably involved in the oxygen transport process of ascidans (sea-squirrels). But the role of vanadium in O_2 transport is still questioned.

5.4 DISTRIBUTION OF OXYGEN CARRYING PROTEINS IN BIOLOGICAL SYSTEM

Iron containing oxygen carriers are present inside the cells and copper containing oxygen carriers are found in extracellular fluids. These iron containing proteins bear **Fe(II)** which can survive inside the cells where a reducing environment exists. Very often, **Fe(II)** gets incorporated within the **macrocyclic porphyrin ligand** to produce the **non-labile Fe(II) complexes**. This porphyrin ligand is **susceptible to oxidative attack**. Thus the reducing environment within the cell protects the porphyrin ring. On the other hand, in the copper containing proteins, **Cu(I)** and **Cu(II)** form very stable complexes with the ligands like imidazole sites from the protein chains. These stable copper-based carriers can survive in bloodstream.

5.5 HEMOGLOBIN (Hb) AND MYOGLOBIN (Mb) IN OXYGEN TRANSPORT MECHANISM

The hemoglobin family is distributed in different living species like vertebrates, invertebrates and annelid worms. The **monomeric unit** is myoglobin. Depending on the structural features they are known as **myoglobin (Mb)**, **hemoglobin (Hb)**, 4 subunits in vertebrate species), **erythrocrucorin (Er)**, 192 subunits in arthropod species), **chlorocruorins (Ch)**, 192 subunits in annelid worms). Mb, Hb and Er use the **Fe(II)-protoporphyrin-IX** (known as **heme b** or **protoheme**) as the basic unit while in Ch, **heme b** unit is replaced by **chloroheme unit** (cf. Fig. 7.5.1.1). On oxygenation, the colour changes as : **purple** \rightarrow **red** (Hb, Mb), **purple** \rightarrow **red** (Er), **purple** \rightarrow **green** (Ch). In this section, Hb and Mb in vertebrate species will be discussed.

5.5.1 Structural Features of Heme Group in Hb and Mb

Fe-porphyrin referred to as heme is the prosthetic group of Hb and Mb. The framework of heme is derived from porphin (Fig. 5.5.1.1), an unsubstituted tetrapyrrole connected at the α -carbons by methyldiene linkages ($=CH-$). Substitution on 8 pyrrole positions on a porphin ring produces a porphyrin ring. Different substitutions on porphin ring at the eight pyrrole positions produce **protoporphyrin IX (PIX)** (Fig. 5.5.1.1) which is used in heme. The porphyrins can donate two protons from each pyrrole ring to form 2- anions. Coordination by the four pyrrole nitrogens of PIX to Fe(II) produces an uncharged heme unit. At biological pH (~7.0), the two carboxyl groups attached to the surface of PIX are ionised and the heme unit is dinegative. **The Fe(II)-protoporphyrin-IX unit is known as heme b.** The chloroheme unit (found in Ch) differs slightly from heme b in substitution (cf. Fig. 7.5.1.1). For both Hb and Mb, the active site contains this heme unit. The fifth position is coordinated by the imidazole nitrogen of proximal histidine (F8) of the globin protein chain. The heme unit cannot itself carry O_2 , but when it is folded with the globin protein, it can perform the task.

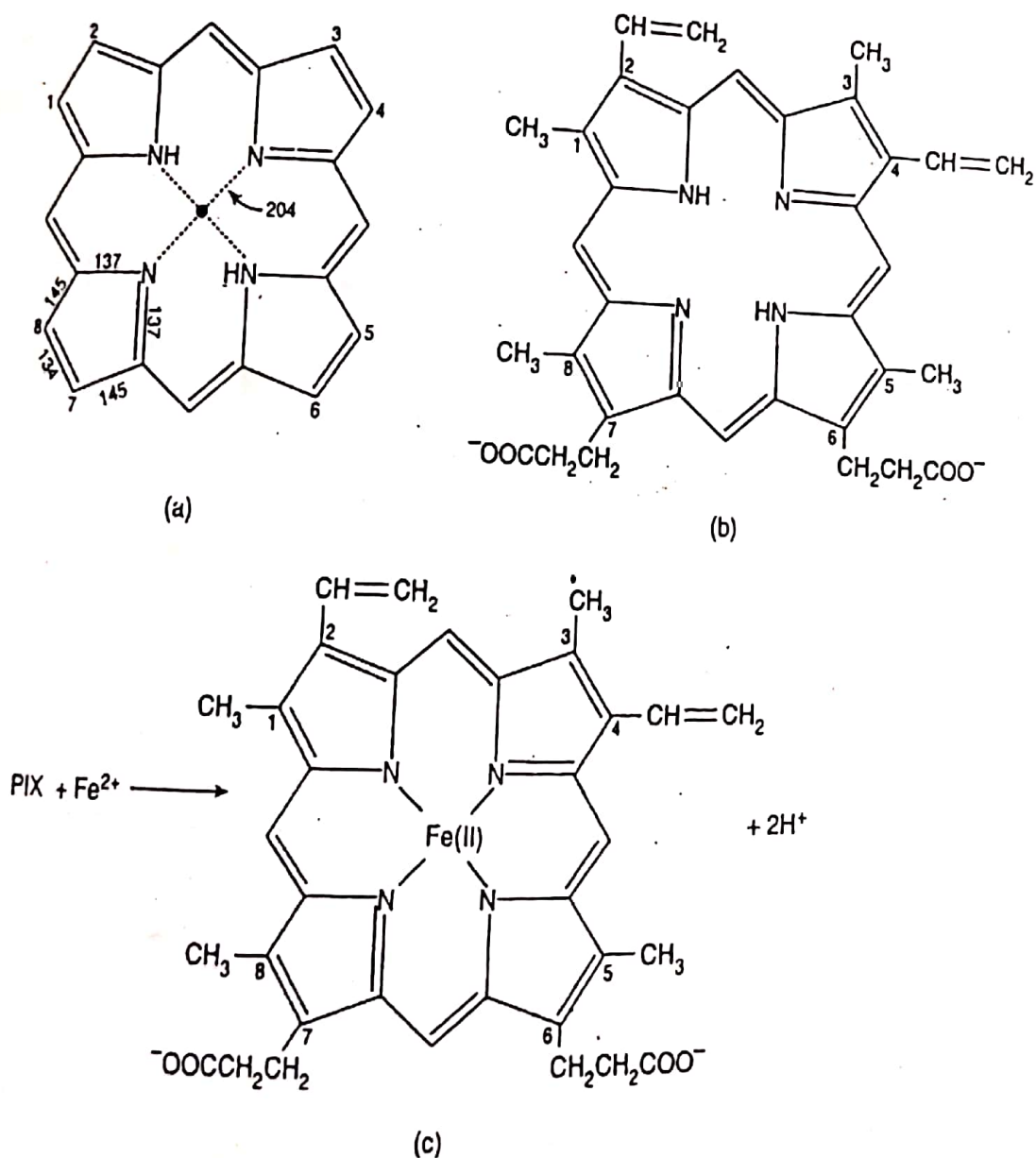
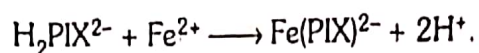


Figure 5.5.1.1: (a) Structure of porphin (bond lengths given in pm). Substituents at the 8 pyrrole positions produce porphyrin. (b) Structure of protoporphyrin IX (PIX). (c) Structure of Fe(II) - protoporphyrin complex (i.e. heme-b)

[**Note :** The $\text{—CO}_2\text{H}$ groups present at the surface of PIX remain dissociated at biological pH. In terms of the number of dissociable protons, the ligand should be represented as H_4PIX where H_4 accounts for two $\text{—CO}_2\text{H}$ group protons and two $>\text{NH}$ group protons. The $>\text{NH}$ protons are lost during complexation with Fe^{2+} . Thus **heme b** is produced in the reaction :



However, for the sake of simplicity, for all forms of the ligand it is simply represented by PIX.]

The important functions of the heme-proteins are: (i) transport and storage of dioxygen (e.g. Hb, Mb); (ii) electron transport (e.g. cyt b_5); (iii) catalysis in redox reactions (e.g. catalase, peroxidase, cytochrome P-450, NO synthase, etc.). All these proteins possess the iron protoporphyrin IX unit as the common prosthetic group in spite of their different biological functions. The protein structure controls these properties. It is illustrated for Hb/Mb (O_2 uptake property) and other proteins (e.g. cyt P-450, catalase, peroxidase, etc) leading to the heterolytic cleavage of O—O bond. The '**push-pull**' mechanism is important for such heterolytic O—O bond cleavage. These aspects have been discussed in Secs. 5.5.7, 7.9.4 and 7.10.

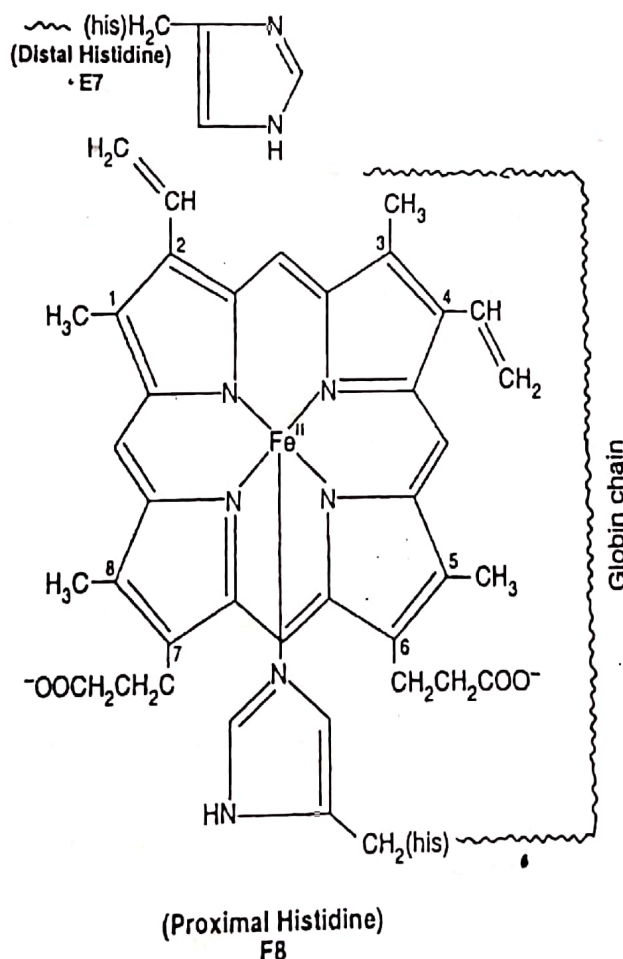


Figure 5.5.1.2 : Structure of a heme unit in hemoglobin and myoglobin.

A heme unit including the globin protein chain is called myoglobin (Mol. Wt. = 16,000 Daltons) (Fig. 5.5.1.2 and 3) and hemoglobin (Mol. Wt. = 64,000 Daltons) is a tetramer of myoglobin subunits. From the standpoint of protein structure, the four units are similar but not identical. The most common hemoglobin in adults contains two α -units (141 amino acid residues) and two β -units (146 amino acid residues) and it is called Hb-A ($\alpha_2\beta_2$). Depending on the amino acid sequence, the protein chains are characterised by α , β , δ and γ . Hb-A₂ ($\alpha_2\delta_2$) is the minor (~2%) constituent of

human blood. In fetus, the fetal hemoglobin is Hb-F ($\alpha_2\gamma_2$). In Hb, these four polypeptide chains are coiled in such a fashion that the four heme units are more or less at the **corners of a tetrahedron** near the surface of the molecule. The protein chains bear $-\text{CO}_2^-$ and $-\text{NH}_3^+$ groups and the chains are coiled to bring about **salt-bridge interactions** (i.e. $-\text{CO}_2^- \cdots \text{H}_3\text{N}^+$, cf. Fig. 5.5.1.5). In Hb-A ($\alpha_2\beta_2$), there are eight such interacting sites in its deoxy-form and these bridges are destroyed on oxygenation.

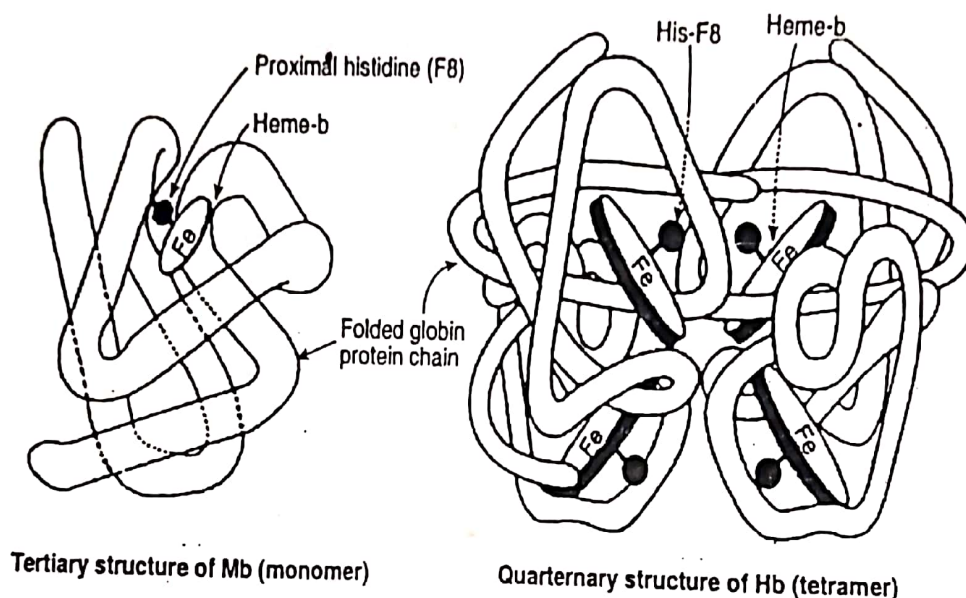


Figure 5.5.1.3 : Structure of myoglobin (Mb) and Hemoglobin (Hb) with the globin protein chain.

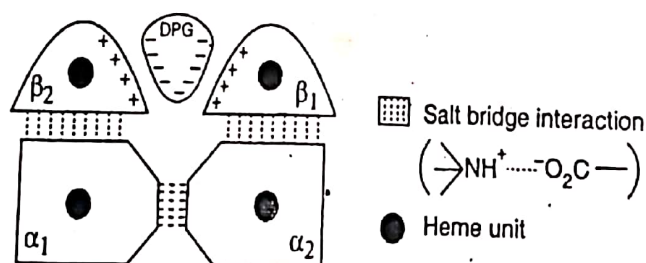


Figure 5.5.1.4 : Schematic representation of tetrameric hemoglobin (Hb-A)

Hb transports O_2 from its source (e.g. lungs, skin and gills) to the site of its biochemical use (i.e. respiration) inside the muscle cells where O_2 is transferred and stored in Mb.

In the planar porphyrin ring of heme unit of Hb and Mb, due to the presence of **conjugated double bonds** in the porphyrin, stable π and low lying π^* orbitals are available and these allow the characteristic **charge transfer electronic transitions** to give the red colour of blood. These transitions occur in the range 400–600 nm giving rise to Soret (400–500 nm) and α , β -bands (500–600 nm). The high energy $\pi-\pi^*$ (near to UV) transition of the iron porphyrin ring system is described generally as **Soret band**. This band is also described as γ -band (cf. cytochromes).

Definition of Soret Band (IUPAC recommendation, 1997) : An intense ($\pi \rightarrow \pi^*$) absorption band in the blue region of the optical absorption spectrum of a heme protein (e.g. Hb, Mb, Cyt, etc.) is called Soret band. Thus the Soret bands appear near the ultraviolet region.

In the Mb and Hb, the sixth coordination site of iron remains vacant or occupied by H_2O deoxy-forms and this site is occupied by O_2 in their oxy-forms. It is worth noting that near sixth coordination site, there is another histidine residue (called *distal histidine*, E7; cf. Fig. 5.5.7.1) which cannot coordinate iron, but it plays a very crucial role to stabilise the oxy-form through bonding (cf. Fig. 5.5.7.1). This distal histidine protects Hb and Mb from CO poisoning aspects have been discussed in Sec. 5.5.7. Properties of the distal moiety largely control properties of different heme proteins, e.g. Hb/Mb, cytochrome P-450, peroxidase, etc. The proximal ligand is important to introduce the 'pull effect' in certain heme proteins. The proximal ligand plays some important roles, e.g. 'push effect'. All these aspects have been discussed in Secs. 5.5.7, 7.9.4 and 7.10. The microenvironment of the iron in Hb and Mb is very comparable with that of cytochrome c but in cyt c all six coordination sites are filled. Their functions are also different : cytochrome c, an electron carrier; Hb, an oxygen carrier.

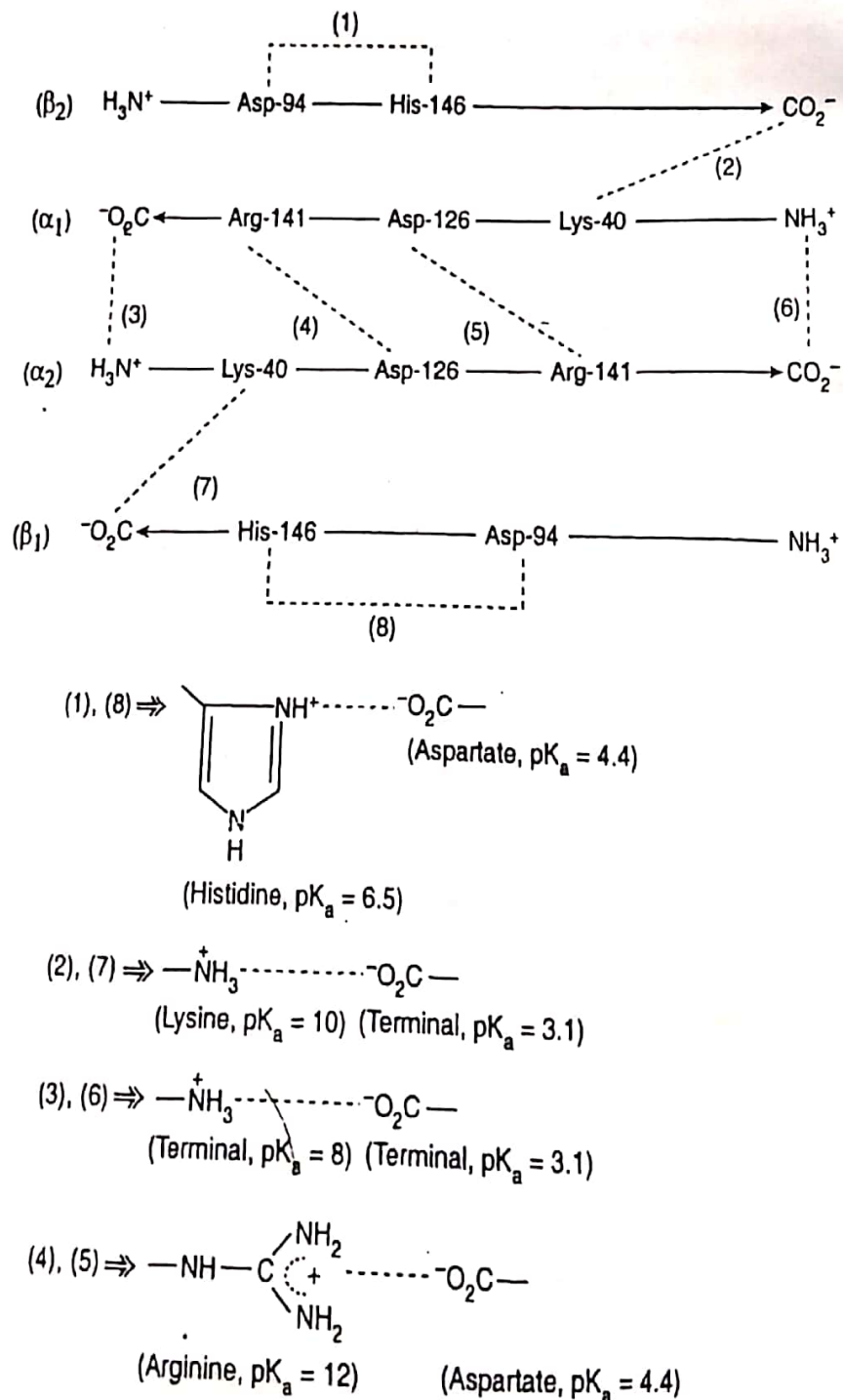


Figure 5.5.1.5 : Salt-bridge interactions in Hb-A ($\alpha_2\beta_2$). Given pK_a values correspond to the respective conjugate acids.

The folded globin protein chains in Hb perform several important tasks. The important structural aspects of the globin protein are worthy to be mentioned. The peptide backbone of the globin protein contains various side chains having nonpolar hydrophobic moieties (i.e. hydrocarbon), cationic (i.e. $-\text{NH}_3^+$) and anionic (i.e. $-\text{CO}_2^-$) sites. The coiled structure of the four polypeptide chains of Hb is stabilised mainly through salt-bridge interactions (i.e. $-\text{CO}_2^- \cdots \cdots +\text{H}_3\text{N}-$) in $\beta_1-\beta_1$, $\beta_2-\beta_2$, $\beta_2-\alpha_1$, $\alpha_1-\alpha_2$ and $\alpha_2-\beta_1$ chains of Hb-A (Fig. 5.5.1.5), hydrophobic interactions among the nonpolar moieties and H-bonding interactions among the peptide backbone units. 2,3-diphosphoglycerate (DPG) (now it is called 2,3-bisphosphoglycerate and is denoted by BPG) having a large number of negatively charged sites can interact with the positively charged residues ($-\text{NH}_3^+$) on both the β -chains (cf. Fig. 5.5.1.4). All these interactions are responsible to give the **quaternary structure** of deoxy-Hb and this form is termed as the **T (tense) form**, but on oxygenation these interactions are destroyed to give the **R (relaxed) form** of oxy-Hb.

Mb (monomeric) has only one oxygen binding site while Hb (tetrameric) has got four oxygen binding sites which interact in a cooperative manner. In deoxy-form, Fe(II) does not properly fit in the porphyrin cavity and it lies about 70 pm above the porphyrin plane in the direction of proximal histidine residue (cf. Fig. 5.5.4.1). Thus approximately a square pyramidal environment (C_{4v} symmetry) is attained in deoxy-Hb, but on oxygenation Fe(II) fits into the porphyrin cavity and travels about 70 pm towards the porphyrin plane. On oxygenation, T (tense) form of deoxy-Hb changes to R (relaxed) form of oxy-Hb.

5.5.2 Function of Hb and Mb

Hemoglobin (Hb) carries O_2 from lungs to tissues where it is transferred to myoglobin (Mb) and stored therein for metabolic requirements. To make this process thermodynamically possible, the oxygen affinity of Hb in lungs where oxygen concentration is high should be greater than that of Mb and the reverse condition should arise in the tissues where oxygen concentration is less. Nature has designed Hb and Mb in such a fashion that this condition is attained automatically (Fig. 5.5.2.1). These are evident from the characteristics of O_2 -binding interaction with Hb and Mb.

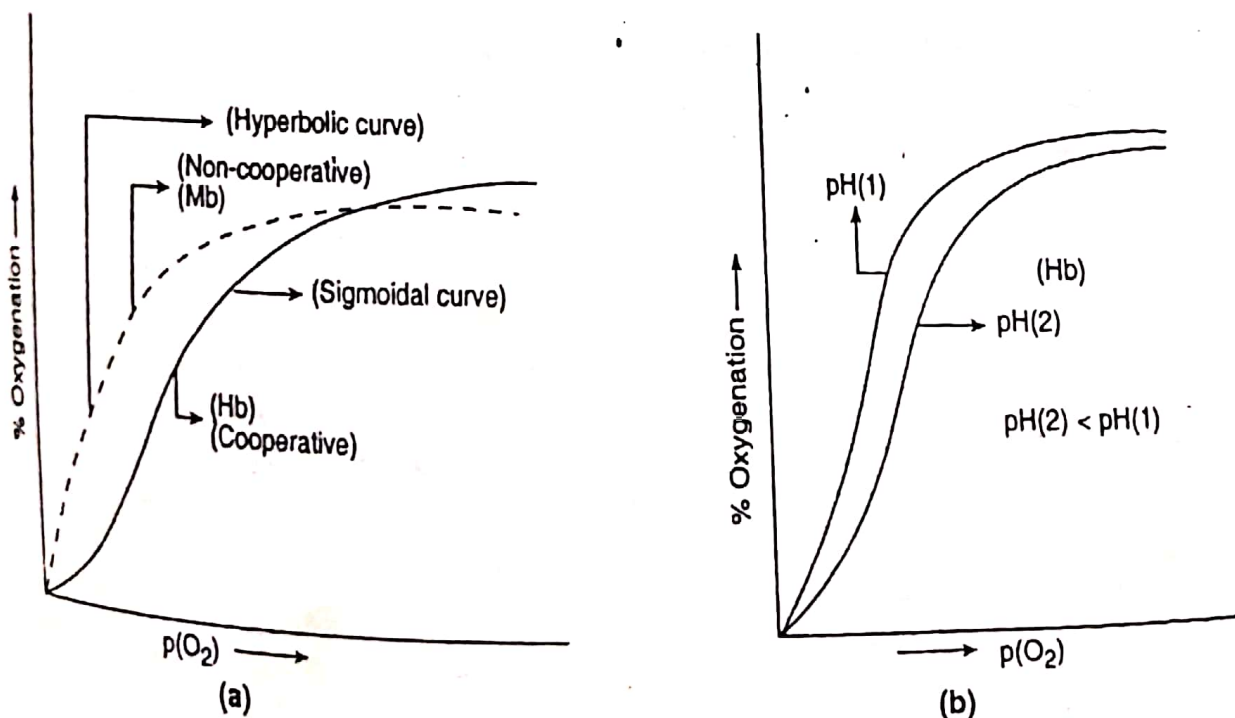


Figure 5.5.2.1: Oxygenation curves for Hb and Mb (a). Effect of pH on oxygenation (Illustration of Bohr effect) of Hb (b). (Qualitative representation)

5.7 HEMERYTHRIN (Hr) – AN OXYGEN UPTAKE METALLOPROTEIN

A large number of marine invertebrates are found to utilise the iron bearing protein – hemerythrin having no porphyrin skeleton in oxygen transport. This **nonheme protein** bears Fe(II) in deoxy-form. When it is oxidised, it forms methemerythrin (Met-Hr) which contains Fe(III) and then it cannot bind oxygen. In Hr, the cooperativity effect on O_2 affinity is insignificant with the Hill coefficient (n) 1.2-1.4 in accord with its role in O_2 storage (cf. Mb with $n = 1$, Mb used in O_2 storage). But in some cases, higher cooperativity has been reported. Hemerythrin can exist in both monomeric (Mol. Wt. = 13,500 Daltons) and octameric (Mol. Wt. = 108,000 Daltons) forms. The trimeric form is also known. The monomeric form is also known as myohemerythrin (cf. myoglobin vs. hemoglobin) which is exclusively used for O_2 -storage. Each subunit contains two Fe(II) centres (high-spin) and deoxy-Hr is paramagnetic. The oxy-Hr is diamagnetic at low temperature through an antiferromagnetic coupling interaction between the Fe(III) centres. The two Fe(II) centres are joined by two bridging carboxylates Glu-58 and Asp-106 of the protein chain. There is also another oxo group ($-O-$) or hydroxo group ($-OH$) to act as the third bridging ligand. One Fe(II) centre is coordinated by three histidine residues (His-101, His-73, His-77) to attain the octahedral geometry, while the other Fe(II) centre coordinates with His-25 and His-54 keeping the sixth site reserved for O_2 binding as **peroxide or hydro-peroxide** ($\nu_{O-O} = 844\text{ cm}^{-1}$). Thus the deoxy-Hr is characterised by: $(\text{His-N})_3\text{Fe}^{\text{II}}(\mu\text{-OH})(\mu\text{-}\eta^1 : \eta^1\text{-O}_2\text{C-Glu})(\mu\text{-}\eta^1 : \eta^1\text{-O}_2\text{C-Asp})\text{Fe}^{\text{II}}(\text{N-His})_2$. Each subunit can bind with one molecule of oxygen (i.e. $\text{Fe} : \text{O}_2 = 2:1$; for Hb, it is 1:1) as shown in Fig. 5.7.1.

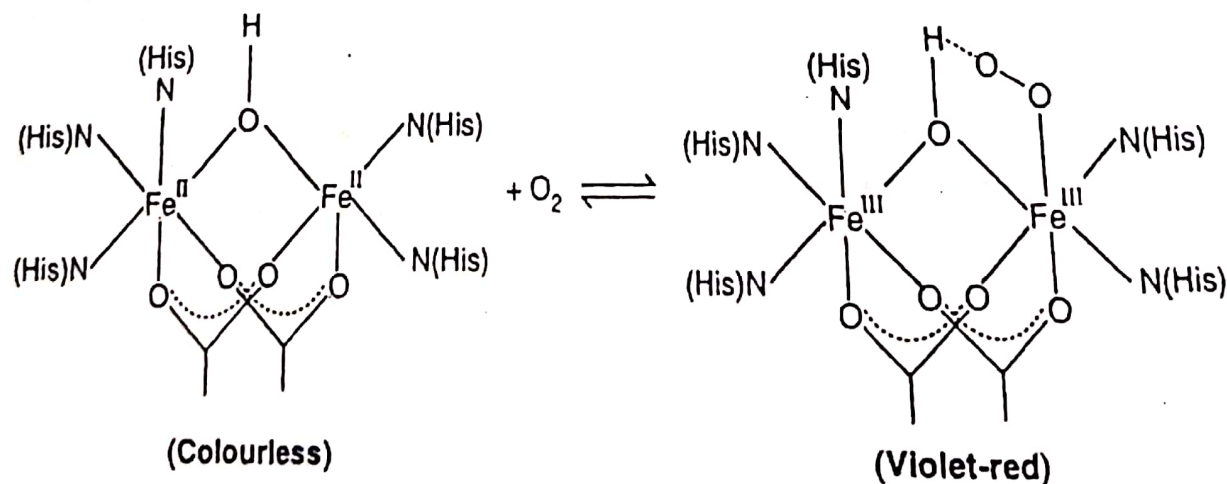


Figure 5.7.1: Structural representation of the mode of O_2 binding in hemerythrin.

Thus, dioxygen binds **asymmetrically as a peroxide** in oxy-Hr and it leads to oxidation of the Fe(II) centers to Fe(III) centers during oxygenation. The O—O stretching frequency supports the existence of peroxo (O_2^{2-}) linkage in oxy-Hr (cf. in oxy-Hb, O_2^- exists). In oxy-Hr, the two Fe(III) centres participate in **antiferromagnetic coupling interaction** to attain the diamagnetism. The deoxy-Hr is colourless, but in oxy-Hr, an intense absorption band arises at 360 nm due to the charge transfer band [$O_2^{2-} \rightarrow Fe(III)$] which looks violet in colour. Here it is important to note that Bohr effect is absent in Hr.

5.8 HEMOCYANIN (Hc) – AN OXYGEN UPTAKE PROTEIN

Hemocyanins are copper containing O_2 uptake proteins, occurring in a number of invertebrates. Depending on the distribution pattern, hemocyanins are classified in two groups, viz. *molluscan-Hc* (found in snails, octopi, etc.) and *arthropodan-Hc* (found in lobsters, scorpions, etc.). Hemocyanin occurs freely in bloodstream (cf. Hb occurs inside the erythrocytes). In the molluscan family, the subunit (containing two Cu(I) centres) has the Mol. Wt. $\sim 53,000$ Daltons, while in the arthropodan family the subunit (containing two Cu(I) centres) has the Mol. Wt. $\sim 77,000$ Daltons. Both types of Hc remain in polymeric forms and the molecular aggregates are composed of 6, 12, 24 or 48 subunits. It is noteworthy that no monomeric form containing one subunit exists for Hc (cf. Mb is a monomer).

For some hemocyanins, the O_2 binding affinity is highly cooperative, with the Hill coefficient as high as $n \sim 9$. Deoxy-Hc containing Cu(I) centres is diamagnetic and colourless, but oxy-Hc is blue (Greek word *cyanos* means blue). Each subunit can bind one O_2 molecule (i.e. $Cu : O_2 = 2 : 1$). The bound O_2 remains **symmetrically** (cf. in oxy-Hr, O_2 is bound **asymmetrically**) bound as shown in Fig. 5.8.1

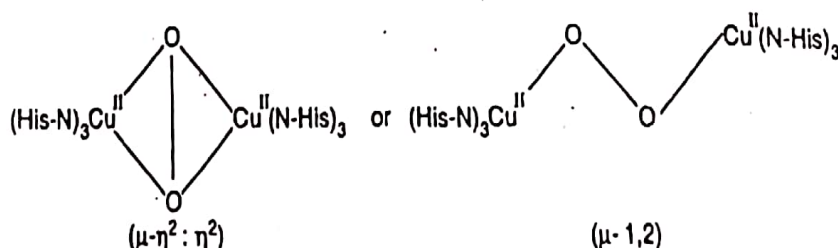


Figure 5.8.1: Structural representation of the mode of attachment of O_2 in oxyhemocyanin.

In oxy-Hc, the O—O stretching frequency is $\sim 744 \text{ cm}^{-1}$. It indicates that the coordinated dioxygen is a **peroxo species** (cf. in oxy-Hr, peroxo species is present and in oxy-Hb, superoxo species is present). Here it should be pointed out that there are different views on the mode of binding of peroxo group with the copper centres. EXAFS (extended X-ray absorption fine structure) data indicate that O_2^{2-} binds **symmetrically** with the Cu-centres as shown in Fig. 5.8.1 [$\mu-\eta^2:\eta^2$ bonding i.e. the bridging unit is $\text{Cu}^{\text{II}}(\mu-\eta^2:\eta^2-\text{O}_2)\text{Cu}^{\text{II}}$; the other possibility involves the bridging unit as $\text{Cu}^{\text{II}}(\mu-1,2-\text{O}_2)\text{Cu}^{\text{II}}$ with a Cu—Cu separation of 360 pm]. Because of the conversion of O_2 to O_2^{2-} the Cu(I) centres become Cu(II) centres on oxygenation (cf. Hr where formation of O_2^{2-} leads to oxidation of Fe(II) centres to Fe(III) centres). The bonding scheme ($\mu-\eta^2:\eta^2$) shown in Fig. 5.8.1 is also supported by studying a model complex containing two Cu(II) centres bridged by η^2, η^2 -peroxide. The similar mode of bridging by the peroxo group has been considered in explaining the activity of tyrosinase (cf. Scheme 7.11.2.1)

The diamagnetic property of oxy-Hc arises due to **antiferromagnetic interaction** between the Cu(II) centres. The oxo-form is also epr silent. The **intense blue colour** of oxy-Hc arises probably

due to charge transfer between the coordinated peroxo group and the metal centre (cf. charge transfer band in oxy-Hr). In oxy-Hc, the charge transfer absorption bands at 580 nm ($\epsilon = 10^3 \text{ M}^{-1} \text{ cm}^{-1}$) and 340 nm ($\epsilon = 10^4 \text{ M}^{-1} \text{ cm}^{-1}$) are due to LMCT (ligand to metal).

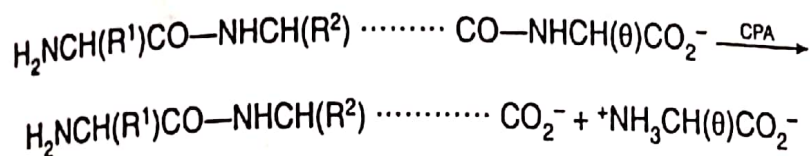
In deoxy-Hc, there are two distorted trigonal coplanar $[\text{Cu}^{\text{I}}(\text{N-His})_3]$ units with the imidazole rings staggered across the Cu Cu separation of 4.6 Å (in horse-shoe crab). In deoxy-Hc, using a bridging ligand (probably H_2O), each Cu(I) center may adopt the distorted tetrahedral geometry. In oxy-Hc, each Cu(II) centre is approximately square pyramid (2 bridging O, 3 His-N; supporting the $\mu\text{-}\eta^2:\eta^2$ structure of Fig. 5.8.1) with a *trans*-axial His-N ligand. This structural change (i.e. distorted tetrahedral or trigonal planar to distorted square pyramidal) during oxygenation is quite significant in explaining the cooperative effect observed for O_2 affinity in hemocyanin.

Note : Comparison of O_2 binding properties of the common O_2 uptake proteins : It is interesting to compare the fate O_2 in Hb, Hr and Hc. In Hr and Hc, the active O_2 -binding site is dinuclear while in Hb, the active site is *mononuclear*. In oxy-Hb, bound dioxygen exists as O_2^- (superoxide) but in oxy-Hr or oxy-Hc, the second metal centre Fe(II) or Cu(I) can provide an additional electron via some metal-metal bridge to reduce further dioxygen to O_2^{2-} (peroxide). The peroxo-moiety is *symmetrically bound* to both Cu(II) centres in oxy-Hc but it is not symmetrically bound to both Fe(III) centres in oxy-Hr. The cooperativity in O_2 binding is measured by **Hill-coefficient** (n) in different O_2 uptake proteins. The approximate values of n are : 3 (for Hb), 9 (for Hc), 1.2-1.4 (for Hr), and 1 (for Mb). Thus in terms of **Hill-coefficient**, Hb and Hc are having the **O_2 transport properties** and Hr is having the **O_2 storage properties** (cf. $n = 1$ for Mb). All these proteins (except Hc) are *paramagnetic* in their deoxy-forms but they are *diamagnetic* in oxy forms. In Hb and Mb, metal : O_2 is 1:1 while in Hr and Hc, metal : O_2 is 2:1.

156 : Carboxypeptidase enzymes are generally activated by different metal ions like Zn(II), Mn(II), Co(II). Both carboxypeptidase-A (307 amino acid residues) and carboxypeptidase-B (308 amino acid residues) require one Zn(II)-site per molecule. But yeast carboxypeptidase-C is not a metalloenzyme.

6.2 CARBOXYPEPTIDASE-A (CPA) : STRUCTURE AND REACTIVITY

These Zn(II)-containing enzymes are released from their inactive precursors or **zymogens** (i.e. procarboxypeptidases) in the pancreas for the digestion of proteins. This pancreatic enzyme is very much specific to hydrolyse the terminal peptide linkage at the carboxyl end. It shows a marked preference towards such peptide linkages in which the side chain of the terminal residue contains some aromatic moiety or branched aliphatic chain with L-configuration (denoted by θ).



The enzyme can also show *esterase activity* (i.e. ester hydrolysis).

6.2.1 Structural Features

CPA exists in different forms (i.e. CPA- α , CPA- β , CPA- γ , etc.) depending on the size of the fragment lost from the zymogen. CPA- α is commonly known as CPA. The prosthetic group of CPA contains a Zn(II) site and the protein bears about 307 amino acid residues. Its molecular weight is 34.6 kDa. CPA- β contains 305 amino acid residues and CPA- γ contains 300 amino acid residues. CPA molecule looks *egg-shaped* and the active site is situated in *cleft* in the protein structure. The Zn(II) centre is coordinated by two N-sites (His-69, His-196), one carboxylate oxygen of the glutamate (Glu-72) and a water molecule (at the fourth coordination site). It provides a distorted tetrahedral geometry around Zn(II). In the vicinity of the active site, the three amino acid residues – protonated guanidyl moiety of Arg-145, phenolic OH of Tyr-248 and carboxylate end of Glu-270 are present and these residues play some important roles for the enzymatic activity. A hydrophobic cavity produced by the apoenzymatic portion is important in housing the hydrophobic group (θ) of the terminal residue of the substrate.

6.2.2 Characteristic Features of CPA Reactivity

(a) **Metal substitution** : Zn(II) can be removed from the enzyme by using the stronger chelating agents like 1,10-phenanthroline. The apoenzyme can be isolated through dialysis against the chelating agent, 1,10-phenanthroline. **The apoenzyme is itself inactive.** But the activity can be restored by adding Zn^{2+} and many other bivalent metal ions like Co(II), Ni(II), Mn(II). In fact, the Co(II)-CPA enzyme is more active than the native enzyme, Zn(II)-CPA. The relative activities (towards both peptidase and esterase activity) of different metal substituted enzymes are given in Table 6.2.2.1. It is interesting to note that the Co(II)-CPA is more reactive than the native Zn(II)-CPA, but nature had to select Zn(II) rather than Co(II) because of the nonavailability of Co. The reactivity order for the hydrolysis of glycyltyrosine by metal ion substituted CPA is : $\text{Mn(II)} \ll \text{Zn(II)} < \text{Co(II)}$. With the increase of M—O bond strength, the carbocationic character of the carbonyl carbon increases. According to the Irving-Williams series, the bond strength changes as : $\text{Mn—O} \ll \text{Zn—O} < \text{Co—O}$. The above bond strength sequence has been supported by M—O stretching frequency. The bond strength sequence explains the peptidase activity sequence.

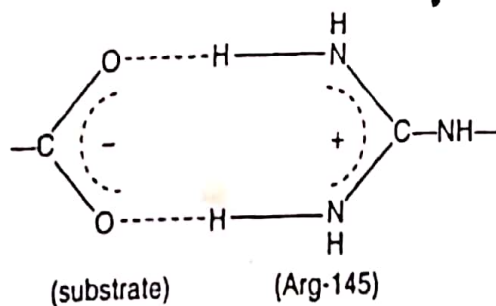
Table 6.2.2.1

Relative activities of different metal-substituted CPA		
Metal	Peptidase	Esterase
Apoenzyme	0	0
Zn(II)	100	100
Co(II)	200	110
Ni(II)	50	40
Mn(II)	30	160
Cd(II)	5	140
Pb(II)	0	60
Hg(II)	0	90

(b) Distorted tetrahedral geometry around Zn(II) - entatic state : To understand the microenvironment and microsymmetry around the metal centre through spectroscopic investigation, Zn(II) (which does not show any $d-d$ transition) is replaced by some comparable transition metals which display the $d-d$ transitions. In the present case, substitution of Zn(II) by Co(II) retains the enzymatic activity. Substitution of Zn(II) (d^{10}) by Co(II) (d^7) allows the spectral studies (*absorption, circular dichroism, magnetic circular dichroism*) of the substituted enzyme. In fact, the Co(II)-substituted enzyme furnishes valuable information about the metal environment. Thus Co(II) serves as an *spectral probe* for the study of the active site. The electronic spectrum of Co(II)-CPA indicates the *distorted tetrahedral symmetry around the metal centre*. In fact, the distorted geometry is also supported by the X-ray studies. Vallee has termed the distorted condition as the '**entatic state**' which is believed to lower the activation energy to attain the transition state.

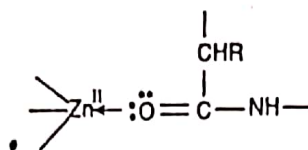
(c) Hydrophobic pocket : This pocket created by the polypeptide chain resides in the vicinity of the active site to house the hydrophobic group (θ) of the terminal residue of the substrate.

(d) Role of Arg-145 in substrate recognition : The *terminal carboxyl group* of the substrate forms a *salt-bridge* (i.e. ionic interaction) with the *protonated guanidyl group* of Arg-145 (Scheme 6.2.2.1). It keeps the substrate in a proper position and orientation as required in the process. This is why, **the enzyme is specific for the terminal peptide linkage at the carboxyl end**. In other words, this salt-bridge interaction helps to recognise the substrate. This interaction also helps the rupture of the N—C bond of the peptide linkage.

**Substrate Recognition**

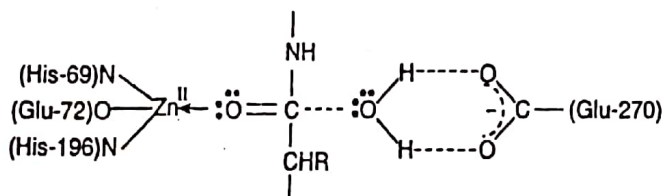
Scheme 6.2.2.1 : Salt-bridge interaction between the terminal carboxyl group of the substrate and arginine-145 in carboxypeptidase-A (CPA).

(e) **Generation of carbocationic character at the terminal peptide carbonyl carbon :** The carbonyl oxygen replaces the H_2O molecule at the active site of Zn(II) . This Lewis acidic character of Zn(II) polarises the ' $\text{C}=\text{O}$ ' bond to develop a carbocationic character on the carbonyl carbon center.



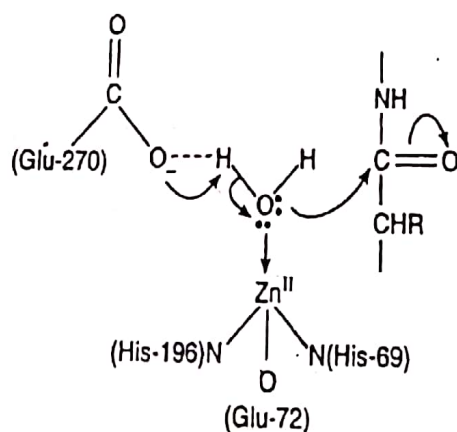
Hydrogen bonding interaction between the $-\text{NH}-$ group (of the peptide linkage) and the phenolic $-\text{OH}$ group of Tyr-248 also enhances the cationic character of the carbonyl carbon and it also helps the rupture of $\text{N}-\text{C}$ bond (cf. Scheme 6.2.2.4). In fact, with the increase of positive charge on the carbonyl carbon centre, the nucleophilic attack on it is facilitated.

(f) **Role of Glu-270 to generate a potential nucleophile :** The carboxylate end of Glu-270 may participate in a number of ways. It can simply keep the nucleophile (i.e. H_2O) in a proper position through hydrogen bonding to help the attack on the target carbonyl carbon (Scheme 6.2.2.2).



Scheme 6.2.2.2 : Correct positioning of H_2O (i.e. nucleophile) through H -bonding interaction of Glu-270 in carboxypeptidase-A (CPA).

The carboxylate group of Glu-270 may interact with the water molecule bound with Zn(II) to generate the metal bound hydroxide group which is a powerful nucleophile to attack the peptide linkage (Scheme 6.2.2.3)



Scheme 6.2.2.3 : Generation of the enzyme-bound OH group (a better nucleophile) by Glu-270 to attack the substrate in carboxypeptidase-A (CPA) activity.

The carboxylate group of Glu-270 can itself act as a good nucleophile to produce an acid anhydride as shown in Scheme 6.2.2.4. In fact, existence of acid anhydride has been proved. The probable enzymatic activity of CPA is outlined in Scheme 6.2.2.4.

7.2 IRON-SULFUR PROTEINS

7.2.1 General Features of the Iron-Sulfur Proteins

The non-heme iron-sulfur proteins (commonly known as **ferredoxins**, sometimes abbreviated as Fd, where *fer* means iron and *redoxin* means redox protein) are extremely important in many biological electron transfer processes and these are available in all living bodies. They play vital roles in *photosynthesis, mitochondrial respiration, nitrogen fixation, in the activity of xanthine oxidase, etc.* Ferredoxins mainly act as *electron transport proteins* in the biological redox reactions.

In iron-sulfur proteins, both the cysteinyl sulfur and inorganic sulfur as S^{2-} are present. The inorganic sulfurs are *labile* as they can be removed as H_2S on acidification. The iron-sulfur proteins are very often represented by $nFe-mS$, where n denotes the number of Fe-cations per protein molecule, S denotes the labile sulfur and m denotes the number of labile sulfur sites per protein molecule.

In all iron-sulfur proteins, Fe^{x+} is approximately *tetrahedrally* surrounded by the sulfur sites, at least one of which is a *cysteinyl sulfur*. Another important aspect is that for a particular value of n , in all $nFe-mS$ proteins which may have different sources, the number of cysteinyl sulfur is the same though the amino acid sequences in the protein chains may be different.

In the electron transport process, the Fe^{3+}/Fe^{2+} couple works and both the oxidised and reduced forms of Fe remain in high spin tetrahedral geometry. The sulfur binding site being *relatively soft* tends to stabilise the lower oxidation state Fe^{2+} of the Fe^{3+}/Fe^{2+} couple. The ionic radii of tetrahedral high spin Fe(III) and Fe(II) differ. This makes the distorted tetrahedral geometry around Fe. During reduction of Fe(III) to Fe(II), this change in ionic radii initiates to change the protein structure (*tertiary and quaternary*). This protein structure change largely

controls the redox potential of the $\text{Fe}^{3+}/\text{Fe}^{2+}$ couple. Thus by varying the protein structure (i.e. amino acid sequence), the reduction potential of the $\text{Fe}^{3+}/\text{Fe}^{2+}$ couple for ferredoxins can be varied in a wide range (-0.6 to + 0.3 V, at biological pH). In iron-sulfur proteins, the **charge transfer (LMCT) band** occurs in the range 350–600 nm due to $\text{S} \rightarrow \text{Fe}$ transition. Properties of some Fe-S proteins are given in Table 7.2.1.1.

Table 7.2.1.1
Some representative Fe-S proteins

Protein	Source	Mol. Wt (kDa)	E_0' (V) at approximately biological pH
Rubredoxin (1Fe)	<i>C. pasteurianum</i>	6.0	- 0.57
2Fe-2S	<i>Spinach</i>	10.6	- 0.42
	<i>Azotobacter</i>	21.0	- 0.35
	<i>C. pasteurianum</i>	25.0	- 0.30
	Pig adrenals (Adrenodoxin)	16	- 0.27
	<i>E. coli</i>	12.6	- 0.36
	<i>Thermus</i>	20.0	+ 0.15
	<i>thermophilus</i> (Rieske)		
4Fe-4S	<i>Bacillus</i>	9.1	- 0.28
	Beef heart (Aconitase active)	81.0	—
	<i>Chromatium vinosum</i> (HiPIP)	10.0	+ 0.35
Xanthine oxidase (8Fe-8S, 2FAD, 2Mo)		30.0	
Succinate dehydrogenase (8Fe-8S, FAD)	Mitochondria	200.0	
NADH dehydrogenase (28Fe-28S, FMN)	Mitochondria	100	
3Fe-4S	<i>Desulphovibrio</i> (Fd II)	6.0	- 0.13
	Beef heart (Aconitase, inactive)	81.0	

Some representative iron-sulfur protein systems are discussed below.

7.2.2 Rubredoxin (Rd)

1Fe-0S : It is actually $(\text{Cys-S})_4\text{Fe}$ having no inorganic sulfur. It is the simplest bacterial iron-sulfur protein referred to as *rubredoxin* (abbreviated as Rd) with a molecular weight of ~ 6 kDa having 50-60 amino acid residues. Here the protein chain is folded to create a *tetrahedral* cavity by four cysteinyl moieties at the centre of which Fe^{x+} resides. It is a *one electron transport agent*

involving the couple $\text{Fe}^{2+}/\text{Fe}^{3+}$ in which both Fe^{2+} ($e^3t_2^3$) and Fe^{3+} ($e^2t_2^3$) remain in high spin states in tetrahedral symmetry. It is noteworthy that the tetrahedral symmetry is distorted in both the oxidised and reduced forms. The reduced form is expected to experience a **Jahn-Teller distortion** but the oxidised form does not experience any **Jahn-Teller distortion**. This is why, it is believed that the distortion is imposed by the ligands (cf. Sec. 7.1.1).

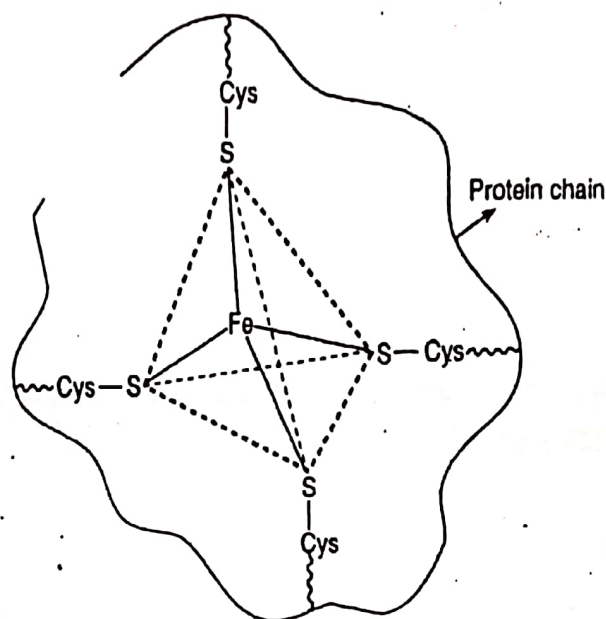


Figure 7.2.2.1: Structural representation of flattened tetrahedral structure of rubredoxin.

This distortion is extremely important for rapid electron transport through an outer sphere process. In fact, this distortion leads to place the Fe-centre in such a geometry that the requirement of structural change during the electron transfer process is minimum. Consequently, according to Franck-Condon principle, the reorganisation energy needed for the outer sphere electron transfer process should be minimum to facilitate the process. In fact, the self electron exchange rate in rubredoxin is tremendously high (ca. 10^9 electron transfer per second). This is mainly due to the fact that the structural parameters (i.e. spin state, geometry, bond angle, etc.) for both the oxidised Rd (i.e. Fe^{3+}) and reduced Rd (i.e. Fe^{2+}) are very much comparable. Here it is important to note that in $\text{Fe}(\text{aq})^{3+}/\text{Fe}(\text{aq})^{2+}$ couple the electron exchange rate is very slow (ca. $1.0 \text{ mol}^{-1} \text{ dm}^3 \text{ s}^{-1}$) where Fe—O bond lengths in $\text{Fe}(\text{H}_2\text{O})_6^{3+}$ and $\text{Fe}(\text{H}_2\text{O})_6^{2+}$ differ considerably. It has been proposed that in rubredoxin the ligand imposed distortion renders the HOMO neither strongly bonding nor anti-bonding thereby facilitating the electron transfer.

In the distorted tetrahedral geometry of Rd, the S—Fe—S bond angle varies in the range 104° to 114° and Fe—S distances range from 224 to 233 pm. When Fe(III) is reduced to Fe(II), there is a slight increase ($\sim 5 \text{ pm}$) in Fe—S bond. The reduction potential of the $\text{Fe}^{3+}/\text{Fe}^{2+}$ couple is about 0.6 V (at pH 7). Different model compounds (e.g. $\text{Fe}(\text{SC}_6\text{H}_5)_4^{1-/2-}$) have been prepared where the 'cys-S' is replaced by thiolate moieties. It has been noted that the magnitude of the dihedral angle between the S—Fe—S plane and the Fe—S—C plane involving the same Fe and S is of an important consideration to determine the redox potential of rubredoxin. This dihedral angle is controlled by the protein structure associated with the Fe-centre.

7.2.3 Ferredoxins (Fd)

(a) **2Fe-2S (2Fe ferredoxin)** : It is also designated as Fe_2S_2 protein. It is a binuclear moiety with two bridging inorganic sulfurs. Here, though there are two iron centres but it acts as a one

electron transfer agent (i.e. in the oxidised form, both the irons are in +3 state while in the reduced form, both Fe^{2+} and Fe^{3+} exist). In both the oxidised and reduced forms, each iron centre remains in high spin state in a distorted tetrahedral symmetry. The diamagnetism (at low temperature) in the oxidised form arises through the antiferromagnetic coupling (i.e. super exchange mechanism) of the $\text{Fe}^{3+}(e^2t_2^3)$ centres through the bridging sulfur sites. On reduction, it consists of both $\text{Fe}^{2+}(d^6)$ and $\text{Fe}^{3+}(d^5)$ centres and because of the odd number of electrons (i.e., $6 + 5 = 11$) the complete quenching of the spins does not occur giving rise to a **doublet paramagnetic state** ($S = \frac{1}{2}$), (i.e., ten electrons are paired through superexchange mechanism but the 11th electron remains unpaired). Thus in the reduced form, the metal centres are nonequivalent (Fe^{2+} and Fe^{3+}) while in the oxidised form both the centres are equivalent (both are Fe^{3+}). It acts as a one electron transport protein as :

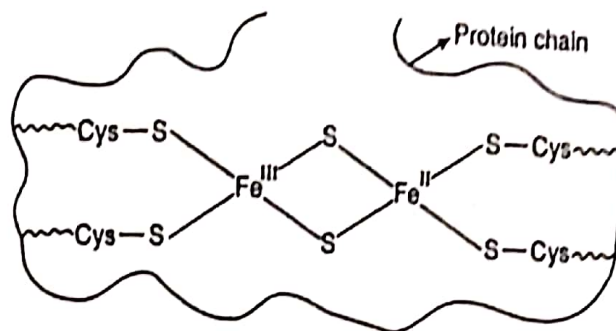
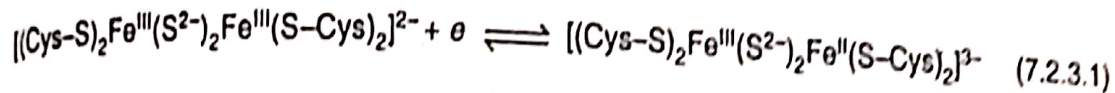


Figure 7.2.3.1 : Structural representation of the active site of 2Fe-ferredoxin (reduced form).

(b) **Rieske Centre (2Fe-2S)** : Rieske proteins belong to the 2Fe-2S class, but at least at one Fe centre Cys-S binding sites are replaced by imidazole N-sites of histidine residues. Ligation by these nonsulfur binding sites remarkably influence the reduction potentials of the $\text{Fe}^{3+}/\text{Fe}^{2+}$ couple. The potentials for the Rieske proteins range from + 0.35 to - 0.15 V (cf. for plant 2Fe-2S ferredoxin proteins, E_0' ranges from - 0.25 to - 0.45 V). Here it is interesting to note that the number of labile S-sites remains unchanged in both ferredoxin and Rieske protein.

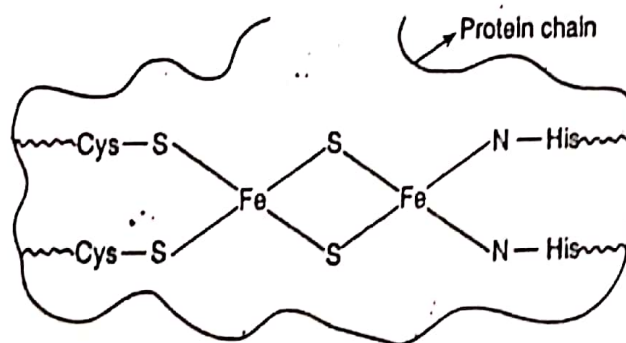


Figure 7.2.3.2 : Structural representation of Rieske iron-sulfur centre.

(c) **4Fe-4S (4Fe-ferredoxin)** : The four iron ferredoxins (designated also as Fe_4S_4 protein) are more well documented than the 2Fe-ferredoxin. Each unit [i.e., $\text{Fe}_4(\text{S-Cys})_4\text{S}_4$] is a **cubane** like cluster of four iron centres and four labile sulfur centres in which each iron centre is coordinated by a cysteinyl residue and other three sites are occupied by three labile S sites. In a distorted cube, 4 alternate corners are occupied by four Fe centres and the other 4 corners are occupied by 4 labile S sites which act as the bridging ligands. The Fe and S centres differ in radii and this is why the cube is

distorted. The "cubane-type" Fe_4S_4 cluster may be considered as the combination of two Fe_2S_2 clusters leading to a tetrahedron of labile S centres cocentric with a tetrahedron of Fe centres. The model compound $[\text{Fe}_4\text{S}_4(\text{SCH}_2\text{Ph})_4]^{2-}$ has been prepared in the reaction of FeCl_3 , NaOCH_3 , NaHS and benzylthiol ($\text{C}_6\text{H}_5\text{CH}_2\text{SH}$) in methanol. The magnetic properties, redox properties, spectral properties of this model compound are very much comparable with those of natural 4Fe-4S ferredoxin.

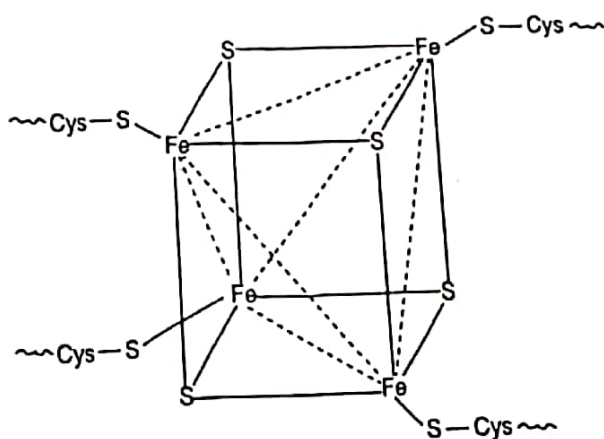
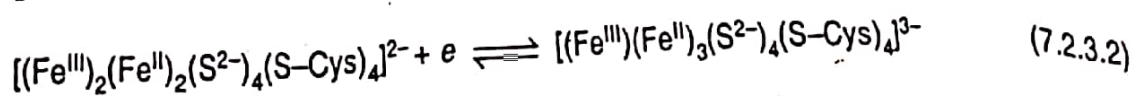


Figure 7.2.3.3 : Structural representation of cubane unit (distorted cube) of 4Fe-ferredoxin.

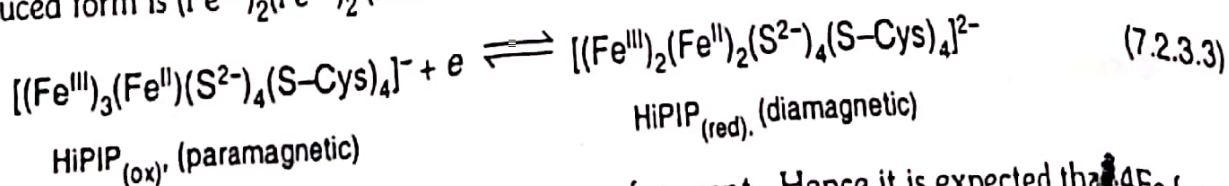
4Fe-4S clusters usually undergo a one electron transfer, but cyclic voltametry studies indicate that it can exist in three forms, i.e. $(\text{Fe}^{3+})_3(\text{Fe}^{2+})$, $(\text{Fe}^{3+})_2(\text{Fe}^{2+})_2$ and $(\text{Fe}^{3+})(\text{Fe}^{2+})_3$. The first and last forms are separated by two electrons. Most of the 4Fe-4S clusters exist as $(\text{Fe}^{3+})_2(\text{Fe}^{2+})_2$ in the oxidised form (diamagnetic) and as $(\text{Fe}^{3+})(\text{Fe}^{2+})_3$ in the reduced form (paramagnetic, $S = \frac{1}{2}$) and the electron transfer process is:



The reduction potential of the couple is -0.4 V at $\text{pH} = 7$. The magnetic properties indicate the existence of antiferromagnetic interaction as in 2Fe-2S protein.

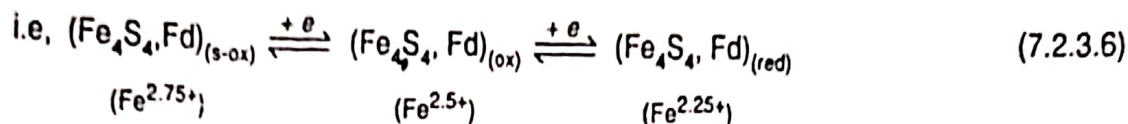
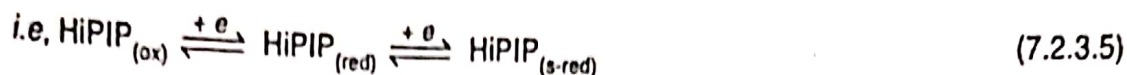
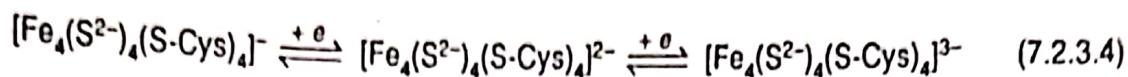
Here it is important to mention that for convenience the different iron centres are designated as Fe(III) and Fe(II), but the experimental evidences indicate that the 4 iron centres are equivalent with some average oxidation state. This equivalent character indicates an extensive delocalisation within the clusters.

There are some 4Fe-4S clusters known as HiPIP (High Potential Iron Proteins known also as clostridial ferredoxin found in *chromatium vinosum*) which also act as a one electron transport protein, but the corresponding reduction potential is very high, approximately $+0.35 \text{ V}$ at $\text{pH} = 7.0$. In HiPIP, it is established that the oxidised form is $(\text{Fe}^{3+})_3(\text{Fe}^{2+})$ (paramagnetic) and the corresponding reduced form is $(\text{Fe}^{3+})_2(\text{Fe}^{2+})_2$ (diamagnetic). The relevant electron transfer process is:



2Fe-ferredoxin acts as a one electron transfer agent. Hence it is expected that 4Fe-ferredoxin should act as a two electron transfer agent. Theoretically it should occur and the cyclovoltametry studies also support this view but the structural effect has got an important role in determining this

aspect. In terms of average oxidation state of Fe-centre, the stepwise electron transfer process among the different possible forms of 4Fe-4S proteins can be represented as :



The reduction potentials at pH = 7 are :

HiPIP : $\text{Fe}^{2.75+}/\text{Fe}^{2.5+}$, $E_0' = 0.35 \text{ V}$; $\text{Fe}_4\text{S}_4\text{, Fd}$: $\text{Fe}^{2.5+}/\text{Fe}^{2.25+} = -0.4 \text{ V}$. The HiPIP is found in *chromatium vinosum* and Fe_4S_4 ferredoxin is found in *peptococcus aerogenes*.

In 4Fe-4S system, the first equilibrium (i.e. $\text{Fe}^{2.75+}/\text{Fe}^{2.5+}$) corresponds to the redox couple of high potential iron protein (HiPIP), while the second step (i.e. $(\text{Fe}^{2.5+}/\text{Fe}^{2.25+})$) corresponds to the redox couple of normal 4Fe-4S ferredoxin. In fact, the form having the average oxidation state $\text{Fe}^{2.75+}$ is the normal oxidised form of HiPIP while it is the *super-oxidised form* of 4Fe-4S ferredoxin, i.e. $(4\text{Fe-4S})_{(\text{s-ox})}$. On the other hand, the form having $\text{Fe}^{2.25+}$ is the normal reduced form of 4Fe-4S ferredoxin while it corresponds to the *super-reduced form* of HiPIP, i.e. $\text{HiPIP}_{(\text{s-red})}$. **In fact, no equilibrium involving $\text{HiPIP}_{(\text{s-red})}$ and $(4\text{Fe-4S, Fd})_{(\text{s-ox})}$ is involved in nature to act as a two electron transport agent in biological system. This is why both HiPIP and 4Fe-4S ferredoxin act as one electron transfer agents in biological system, and the agents utilise different redox couples.**

(d) 3Fe-4S Ferredoxin : Fe_3S_4 cluster protein can be considered as a Fe_4S_4 cubane-type cluster where one Fe centre is missing from one corner of the distorted cube. This is why, 3Fe-4S Fd is described as "*void-cubane*" or "*Fe-depleted cubane*" protein. On addition of Fe^{2+} or other M^{2+} , the vacant corner of the cube is filled in to restore the cubane-type structure.

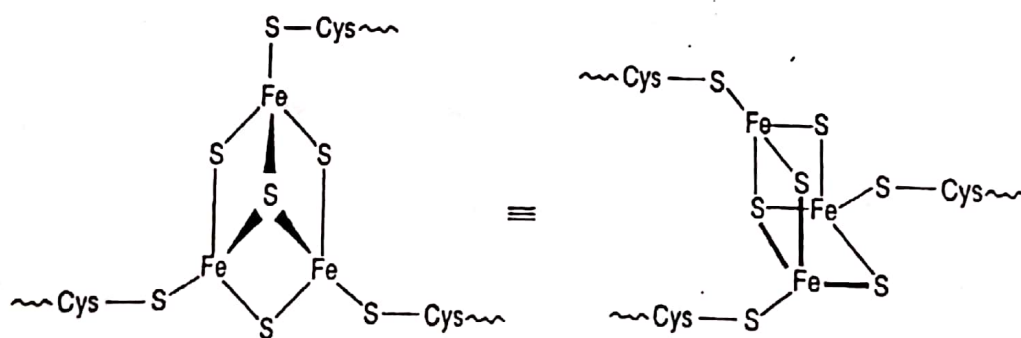
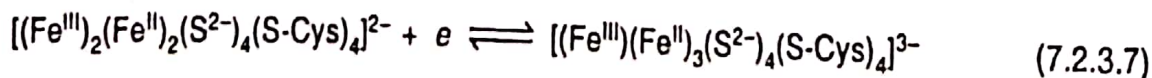


Figure 7.2.3.4 : Active site structure of 3Fe-4S proteins (R = cys).

(e) 8Fe-8S Ferredoxin : Fe_8S_8 cluster consists of two Fe_4S_4 cluster units separated by about 12 Å. Each Fe_4S_4 unit can act as a one electron transfer centre just like the 4Fe-4S ferredoxin.



Thus, as a whole the 8Fe-8S ferredoxin can function as a **two electron carrier**.

The two Fe_4S_4 cubes are linked through protein chains. The cysteine residues at the positions 8, 11, 14 and 45 and four labile sulfur sites coordinate the Fe sites of one cube while the cysteine residues at the positions 18, 35, 38 and 42 and four labile sulfur sites coordinate the Fe centres of the other cube.

In nitrogenase enzyme, the so called *P clusters* present consist of two Fe_4S_4 units, but these Fe-S proteins in P-clusters are different from the common ferredoxin Fe-S proteins (cf. Sec. 8.3).

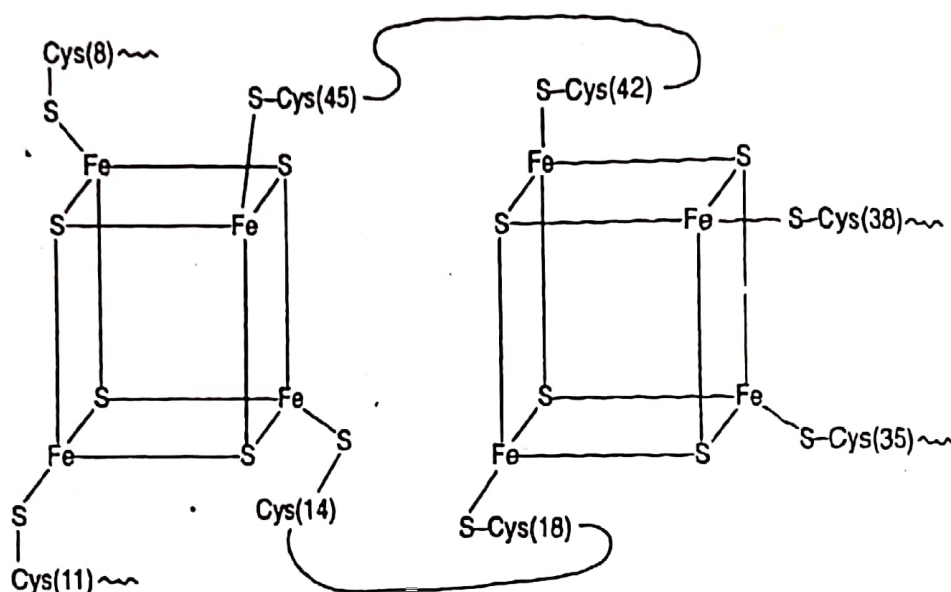
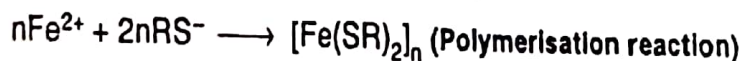
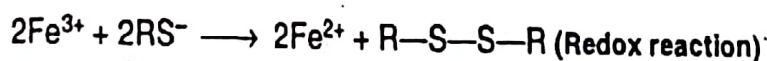


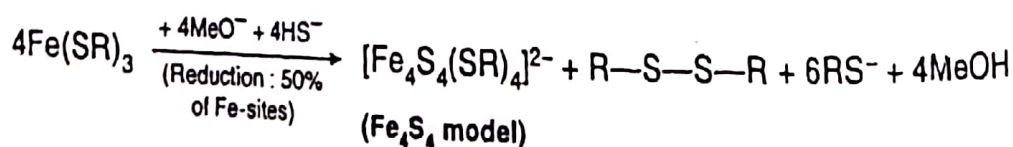
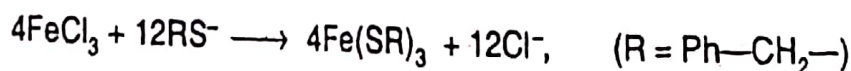
Figure 7.2.3.5 : Structural representation of the active site of 8Fe-8S ferredoxin (the cubes are actually distorted).

7.2.4 Fe-S Model Compounds

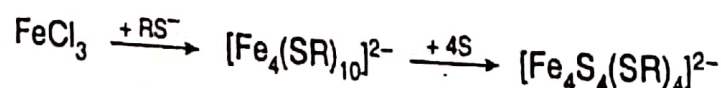
Several model compounds have been synthesised to understand the properties of the Fe-S proteins. Because of the **redox decomposition of the Fe^{III} -thiolate group**, it appeared a formidable challenge (cf. difficulty in the synthesis of model compounds of *Blue proteins* having the Cu^{II} -thiolate group, Sec. 7.3.1) to synthesise the model compounds of iron-sulfur proteins. The redox and polymerisation reactions are :



However, it was overcome by using NaSCH_2Ph in methanol to react with FeCl_3 in presence of NaHS .



The Fe_4S_4 model compound can also be prepared as follows in presence of excess thiolate (3.5 times),



7.5 CYTOCHROMES (cyt)

7.5.1 Structural Features and Classification of Cytochromes

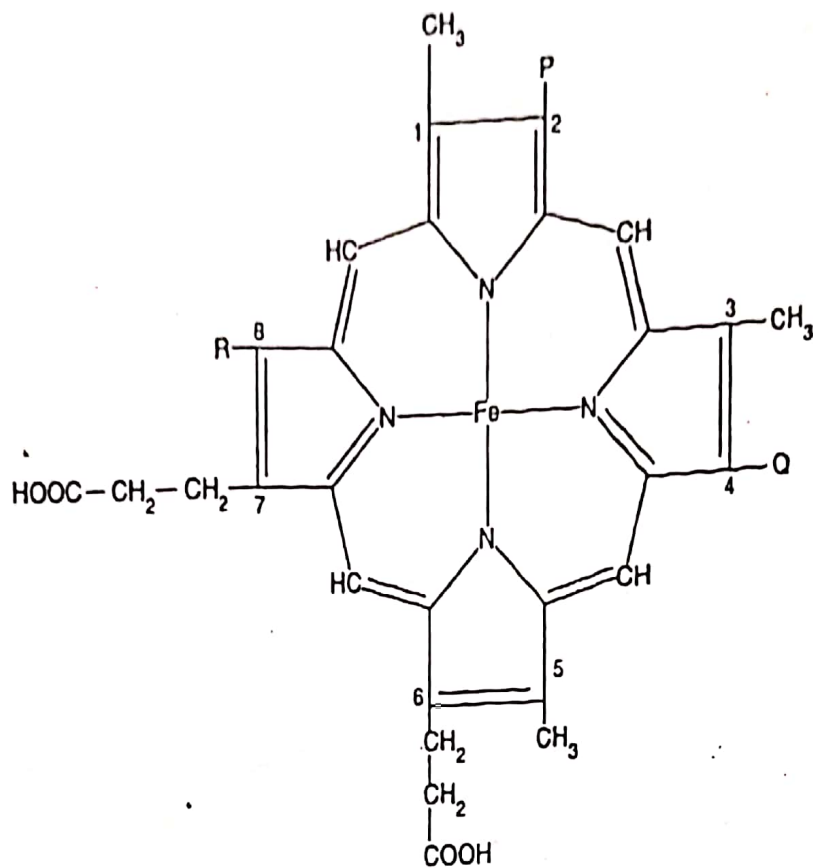
Cytochromes are the most widely distributed metalloproteins (iron-based systems) in carrying out the electron transfer activity in living system. In fact, they are found in all aerobic forms of life. A cytochrome contains one or more heme prosthetic group(s). Cytochromes mainly exist in the membranes of cell mitochondria and chloroplasts to facilitate the electron transfer reactions. The cytochromes are primarily attached to the inner wall of the cell, though to some extent in the cell solution (i.e. the cytosol).

In cytochromes, the active prosthetic group contains the heme group (i.e. iron-porphyrin unit). The pyrrole nitrogens of porphyrin provide a rigid square planar coordination for Fe and the extensive π -system in porphyrin skeleton may itself participate in the electron transfer process. The fifth and sixth coordination sites (i.e. axial positions) may be occupied by the suitable ligating sites coming from protein chain or substrate to give the octahedral geometry of Fe. Cytochromes function by shuttling Fe between Fe(II) and Fe(III) states at the active site and each heme unit can account for one electron transfer activity. In general, the cytochromes are described as one electron transfer reagents in biological systems.

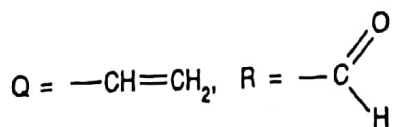
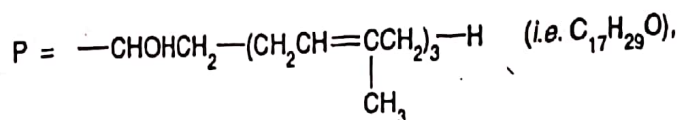
In summary, the essential structural features of cytochromes are : (i) the basic Fe-protoporphyrin IX unit may be substituted around its periphery by different organic groups, varying somewhat from one system to another, (ii) Fe is octahedrally coordinated with the axial ligands below and above the porphyrin plane, often histidine-N but sometimes methionine-S or other protein chains; some cytochromes keep the sixth coordination site vacant for coordination by O_2 ; (iii) the heme unit is bound by one or both of these axial ligands to a protein chain to provide the required hydrophobic environment. The cytochromes present in different organisms differ only in details of the amino acid sequence of the protein chain, but the basic heme unit has been retained throughout the evolution over a billion years for a variety of organisms ranging from, yeast \rightarrow plants \rightarrow lower animals \rightarrow man.

Cytochromes have been classified as **cyt a**, **cyt b**, **cyt c**, etc. based upon the nature of porphyrin ring system and spectral data. The most commonly occurring hemes (Fig. 7.5.1.1) are of three types : **heme a** possessing a long **phytyl tail** ($C_{17}H_{29}O$) is present in the class of cyt a; **heme b** is found in the class of cyt b; **heme c** covalently bound via two thioether linkages is found in the class of cyt c. For the b- and c-types of cytochromes, the prosthetic group is Fe-protoporphyrin IX (found in Hb and Mb); but in cyt b, the prosthetic group is not covalently bound to the protein, whereas in cyt c, the heme unit is covalently bonded to the protein chain by thioether linkages (cf. Fig. 7.5.2.1). These linkages are formed by the addition of —SH groups of cysteine residues to the vinyl ($—CH=CH_2$) groups at the 2 and 4 positions (cf. Fig. 7.5.2.1). For the cyt a, heme a is produced from heme b by replacing one $—CH_3$ group (at the position 8) by a formyl group ($—CHO$) and one vinyl group (at the position 2) by a hydrocarbon chain. There is also another type heme group known as **chloroheme** (found in chlorocruorin).

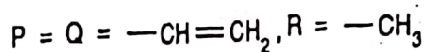
In terms of spectral properties among the different UV-visible absorption peaks (α , β and γ) of the reduced cytochromes (i.e., Fe^{II} -cytochromes), the α -peaks vary characteristically. For example, a-type bears the λ_{max} of the α -band in the longer wavelength region > 570 nm; b-type has the λ_{max} of the α -band in the range 555-565 nm and c-type has the λ_{max} of the α -band in the range 548-554 nm. Thus, the designation, cyt c_{551} for example clearly explains its class. The γ -bands (**Soret bands**) are : 439 nm, 429 nm and 415 nm for cyt a, cyt b and cyt c respectively.



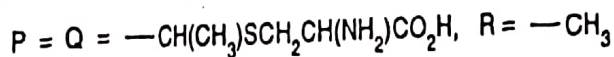
Heme a



Heme b (i.e. protoheme or protoporphyrin IX)



Heme c



Note : The P and Q moieties are linked covalently to the protein chain through cystein residues.

Chloroheme

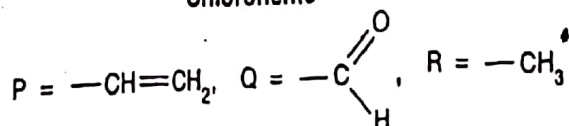


Figure 7.5.1.1: Structural representation of heme a, heme b and heme c groups (active sites) in different cytochromes and chloroheme group in chlorocruorin.

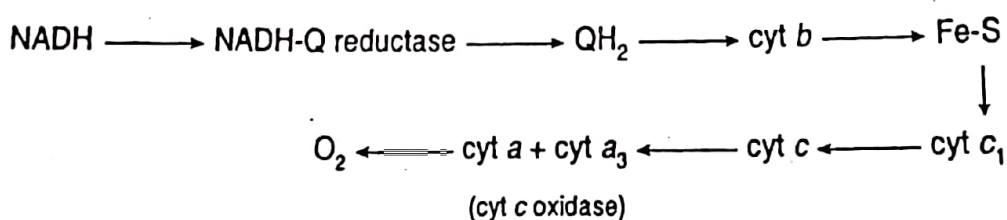
Heme a is found in cyt a; heme b is found in hemoglobin, myoglobin, catalase, peroxidase, cyt b, etc; heme c is found in cyt c; and chloroheme is found in chlorocruorin (an oxygen uptake protein found in annelid worms).

To provide the octahedral geometry around Fe in cytochromes, the 5th and 6th positions are very often *trans*-axially coordinated by the amino acid residues of protein chain. Sometimes, one axial

position is kept vacant (as in cyt a_3) to accommodate the reactant. In cyt a , these two axial positions are occupied by the N-atoms of histidyl imidazole moieties. In cyt c , the axial positions are occupied by the imidazole N-atom of histidine-18 and thioether S-atom of methionine-80 (cf. Fig. 7.5.2.1).

In cytochromes, generally one heme unit exists per molecule but in cyt c_3 (found in a restricted class of sulfate-reducing bacteria), four heme units exist, each ligated by two axial histidines. The reduction potentials of cytochromes may vary from -0.3 V (as in cyt c_3) to $+0.3$ V (as in tuna cyt c) and molecular weight may vary from 13 kDa to 200 kDa.

In the respiratory chain (Sec. 8.1), the electron carriers between QH_2 and O_2 are all cytochromes apart from one iron-sulfur (Fe-S) protein.



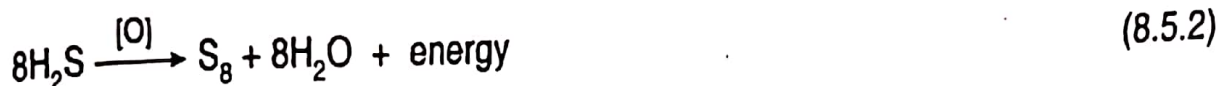
In many other electron transport chains (e.g. photosynthesis), cytochromes play also similar roles. Here we shall discuss cyt c , cyt c oxidase and cyt P-450 in detail.

Fe remains in high spin state for both the oxidised [i.e. Fe(III)] and reduced [i.e. Fe(II)] forms of cyt c . The hydrophobic environment (lower dielectric constant) of the heme unit makes the reduction potential (0.25 V at pH 7) of the Fe(III)/Fe(II) couple more positive compared to that of the same heme complex in aqueous media. Thus it is energetically more costly to oxidise the heme unit (i.e. $\text{Fe}^{\text{II}} \longrightarrow \text{Fe}^{\text{III}}$) in the hydrophobic environment. X-ray structures of the oxidised and reduced forms of cyt c are very much similar. It does not have any vacant coordination site to participate in an inner sphere mechanism for electron transport. It is believed that the electron transfer occurs through the π -system edgewise in an outer sphere mechanism.

Cytochrome c is the oldest biological chemical compound evolved more than 1.5 billion years ago and it is widely distributed in the biological world. The different cyt c from different sources mainly differ in the amino acid sequence of the polypeptide chains. In fact, a family tree of the evolution process from lower animal to higher animal can be constructed in terms of the amino acid sequence of the protein chain in cyt c . In spite of these differences, it has conserved its function and basic structural features throughout the evolution process. It is evidenced by the fact that cyt c from any species will react in other species. The absorption spectra of cyt c from different sources are also comparable. Among the 104 amino acid residues, some residues are invariant for different sources.

8.5 PHOTOSYNTHESIS AND CHLOROPHYLL

All living organisms depend directly or indirectly on *photosynthesis* to capture energy from solar radiation. But there are some *nonphotosynthetic processes* (relatively unimportant) based on *inorganic reactions*, as sources of energy. But these reactions utilise oxygen which is believed to be totally originated through photosynthesis. **Chemolithotropic bacteria** ('rock-eating bacteria') utilise the following reactions (see Sec. 3.2.4 dealing with microbiological mining process) for their required energy.



Nitrifying bacteria utilise the following reactions for energy.



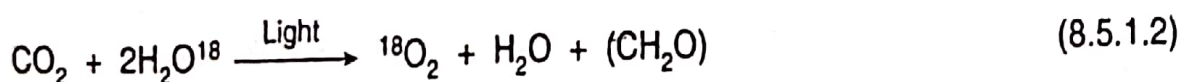
8.5.1 Photosynthesis

Photosynthesis is a redox reaction where H_2O is oxidised to O_2 and CO_2 is reduced to CH_2O (which simply represents carbohydrate), i.e.

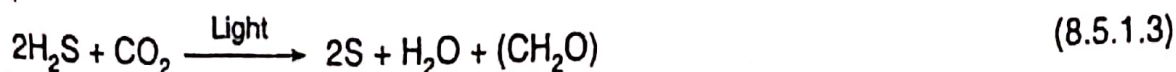


In this process, solar energy is stored as chemical energy. In the respiration, the reverse reaction operates. Photosynthesis in green plants occurs in *chloroplasts* which possess *chlorophylls* to absorb light. Then the light energy is converted into chemical energy through a series of reaction.

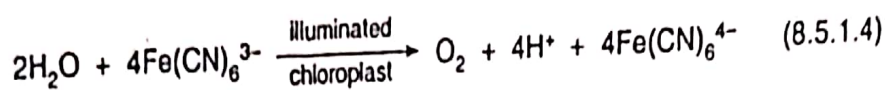
From isotope labeling experiment, it has been proved that the evolved oxygen comes from H_2O not from CO_2 . Thus the reaction should be represented as :



Some anaerobic photosynthetic bacteria use H_2S (instead of H_2O) and produce S.



In fact, in the photosynthetic redox reaction, different electron donors (e.g. H_2O , H_2S , etc.) and different electron acceptors (e.g. CO_2 , NO_3^- , etc.) may be used. But, commonly, the photosynthesis reaction means the involvement of H_2O as an electron donor and CO_2 as an electron acceptor. Robert Hill showed that the isolated chloroplasts on being illuminated can evolve O_2 and reduce an artificial electron acceptor like $\text{Fe}(\text{CN})_6^{3-}$.



This **Hill reaction** proves that O_2 evolution can occur even in the absence of CO_2 and an artificial electron acceptor can substitute CO_2 .

8.5.2 Light Phase and Dark Phase Reactions in Photosynthesis

The overall photosynthesis reaction occurs in two phases. The *light phase reaction* involves the capture of light by *light absorbing pigments* which consequently lead to oxidation of H_2O to O_2 with the concomitant reduction of NADP^+ to NADPH (reduced nicotinamide adenine dinucleotide phosphate). It also leads to the synthesis of ATP .

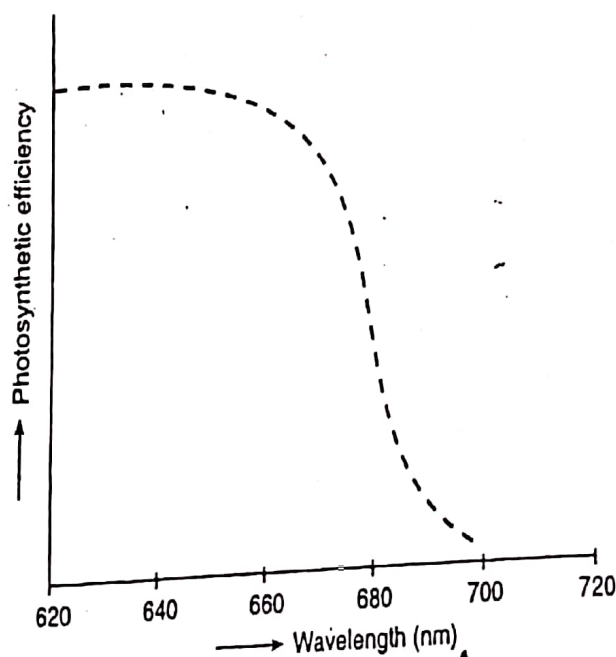
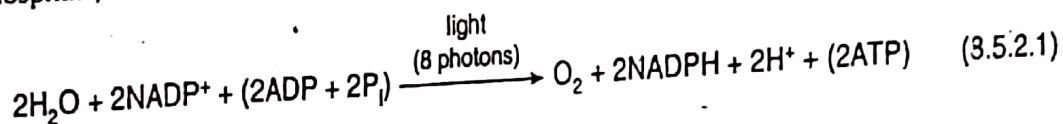
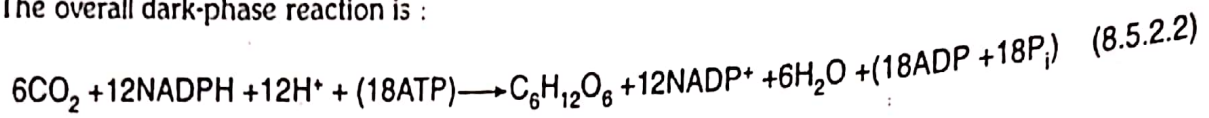


Figure 8.5.2.1: Dependence (qualitative) of photosynthetic efficiency (measured by quantum yield for O_2 evolution) on the wavelength of the illuminating light.

It has been noted that the efficiency of the light phase reaction measured by quantum yield for O_2 evolution does not vary significantly with the wavelength of illumination in the range 400 to 675 nm, but it abruptly decreases for the light of wavelength above 680 nm (Fig 8.5.2.1). This phenomenon is described as **red drop**. This red drop is quite unexpected as Chl-a is known to absorb light in the region of 700 nm (i.e. far-red light). However, the efficiency of the process for the light of 700 nm increases synergistically (i.e. much above the additive efficiency) in the presence

of shorter wavelength light (such as yellow-green light). This observation indicates (as proposed by Emerson) that the two reaction centres are involved in the overall process. In fact, two photosystems (PS-I and -II) are involved in a Z-scheme (cf. Sec. 8.5.5). The dependence of photosynthetic efficiency on the wavelength of light indicates that both the photosystems may be activated at shorter wavelength (< 680 nm) but at higher wavelength (> 680 nm) only one photosystem is activated. In fact, PS-II is activated by the light of wavelength < 680 nm while PS-I is activated by the light of wavelength < 700 nm.

In the dark phase, NADPH reduces CO₂ to carbohydrate with the simultaneous consumption of ATP. This **dark phase reaction** is a complicated one and very often described by **Calvin cycle**. The overall dark-phase reaction is :

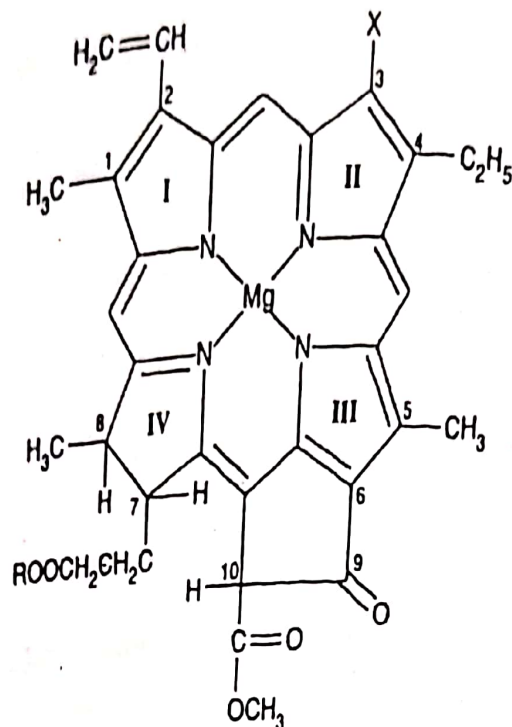


8.5.3 Chlorophylls (Chl) : Structural Features

In the photosynthetic systems, the active component is the green pigment, chlorophyll. Chlorophyll is a macrocyclic complex of Mg(II). Chlorophyll consists of a macrocyclic tetrapyrrole system (Fig. 8.5.3.1) belonging to the porphyrin family with some modifications to the porphyrin ring. The macrocyclic ring in chlorophyll is referred to as **chlorin ring**. Chlorin ring differs from porphyrin ring in several aspects: (i) one double bond in a pyrrole ring (denoted by IV) is reduced; (ii) porphyrins with the reduced tetrapyrrole ring systems are in general known as chlorins; (iii) a cyclopentanone ring is fused to one pyrrole ring (denoted by III); (iii) both the acid side chains are esterified (cf. in heme, the acid side chains remain free). One side chain (attached with the cyclopentanone ring) is a methyl ester while the other chain (attached with the ring IV which is partially reduced) is an ester of **phytol** (C₂₀H₃₉OH). This long chain alcohol is a **tetraisoprenoid alcohol**. In fact, presence of this phytol chain makes chlorophyll highly hydrophobic and soluble in nonpolar media. In ring II, X differs for chlorophyll-b (X = -CHO) and chlorophyll-a (X = -CH₃). The most abundant chlorophyll, chlorophyll-a was first synthesised by Woodward in 1960.

Mg(II) sits at the centre of the chlorin ring and it lies above the macrocyclic plane by ~30 to 50 pm (cf. in oxy-hemoglobin protein, iron sits at the centre of porphyrin ring). Sometimes, chlorophyll is described as a **magnesium porphyrin** in analogy with the heme which is an iron porphyrin. Here it is important to mention that iron plays a crucial role in the biosynthesis of chlorophyll through *template reaction*. Probably, Fe(III) brings the four pyrrole rings in a correct position for condensation to produce a cyclic planar porphyrin ring and it remains as a Fe(III)-chelate. After this biosynthesis, Fe(III) is replaced by Mg(II) which is more abundant. Though the Fe(III)-chelate is more stable, the substitution by Mg(II) is favoured because of two facts : abundance of Mg(II) and crowd of pyrrole rings standing in a queue displaces the iron from the porphyrin complex to utilise the iron for the formation of a new porphyrin ring.

Ultraviolet light is absorbed in atmosphere by O₃ and O₂; infrared light is absorbed by CO₂ and H₂O vapour. The rest portion of the solar spectrum reaching the earth nicely matches with the absorption spectra of the chromophores (e.g. chlorophylls absorb red and blue light; phycocyanin absorbs yellow light; phycoerythrin absorbs blue and green light, carotenoids absorb in the range 410-490 nm range) present in the photosynthetic system.



R = phytyl group; X = $-\text{CH}_3$ (chlorophyll a); X = $-\text{CHO}$ (chlorophyll b)

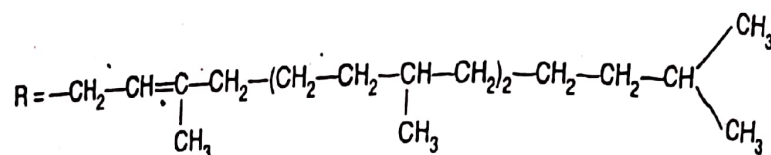


Figure 8.5.3.1 : Structural representation of chlorophyll a and b.

The chlorophyll acts as the **chromophore** in photosynthesis. The extensive conjugation in the chlorin ring allows the electron transition, $\pi(\text{HOMO}) \rightarrow \pi^*(\text{LUMO})$, in the visible region. The peaks are highly intense (extinction coefficient $\approx 10^5$, among the highest values observed for organic compounds). One absorption band arises in the region 430 – 480 nm (i.e. blue light) while the other band appears in the region 645 – 680 nm (i.e. red light). Chlorophyll looks green because it absorbs red and blue light. In the gap, 500-600 nm, the absorption by chlorophyll is relatively weak. However, enough solar energy is absorbed in the blue and red parts of the spectrum. Other pigments like yellow **carotenoids**, and blue or red pigments (**phycoerythrin** and **phycocyanin**) can also absorb light. All these pigments collectively can absorb most of the sunlight. These light harvesting pigments act as **molecular antennas** to absorb the solar energy which is transferred to a centre where the chemical reaction goes on. This reaction site is called **reaction centre** which occupies a very small region in the **photosynthetic unit**. Thus, the function of most of the light harvesting pigments is to absorb light and only a small portion of the chlorophylls present in the reaction centre converts the solar energy to chemical energy. The structural features of the chlorophylls in reaction centre and in antenna have been discussed later (cf. Sec. 8.5.6).

The light harvesting pigments not only facilitate the photosynthesis process but also protect the biological system from the photochemical damage by absorbing the solar radiation.

Extensive conjugation in the chlorin ring of chlorophyll allows the absorption to occur in the visible region (cf. particle in a box model). This conjugation makes the ring rigid and consequently less energy is wasted due to molecular vibration.

8.5.4 The Role of Mg(II) in Chlorophyll

- The choice of Mg(II) in chlorophyll is really unique. In fact, without magnesium the chlorin ring is **fluorescent** (i.e. the absorbed light energy is emitted back immediately). But, after

4260 :
incorporation of Mg(II), chlorophyll becomes **phosphorescent**. This change (due to metal incorporation), i.e. fluorescent to phosphorescent, is biologically very important. If the fluorescence occurs exclusively, the absorbed light energy is lost immediately and it will not be available for chemical transformation in a chemical reaction. Hence, the absorbed light energy must be stored for some while so that it can be utilised in a chemical reaction for the conversion, light energy to chemical energy. For this phosphorescence behaviour, there must be an excited state of finite life-time. Probably, mixing of the excited singlet and triplet states through spin-orbit coupling in magnesium gives a relatively stable triplet excited state. In fact, triplet to singlet transition is not allowed and it makes the triplet excited state stable.

- Mg(II) (d^0 system) does not have any crystal field stabilisation energy to prefer the square planar geometry, rather it prefers the tetrahedral geometry where the steric hindrance is less. But the rigid chlorin ring enforces Mg(II) to have the planar geometry. Consequently, the Mg(II)—N bonds remain in a strained condition, and the electrons constituting the bonds can, therefore, be readily excited by the absorption of light energy. This absorbed energy can be utilised in the desired chemical reactions.

- Through coordination by the chlorophyll to the Mg(II)-centre, **rigidity of the macrocyclic structure is further strengthened**. It may be noted that the macrocyclic ring experiencing conjugation or delocalisation of π -electron cloud is itself sufficiently rigid. The rigidity of the system minimises the energy loss due to molecular vibration (i.e. thermal vibration).

- Stacking of chlorophylls (i.e. polymerisation) in **antenna chlorophyll** i.e. $(Chl)_n$ is attained through the bridging action of Mg(II) between the adjacent chlorophyll moieties (cf. Fig. 8.5.6.1).

- The water molecule coordinated to the Mg(II)-centre in the axial direction in the **chlorophyll of active reaction centre** i.e. $(Chl \cdot H_2O \cdot Chl)$ experiences the **photoinduced splitting** to generate the H-atom that provides the electron for the photosynthetic process. Thus coordination of the water molecule to the Mg(II)-centre plays a crucial role (cf. Fig. 8.5.6.2).

- Here it is interesting to note that for the electron transfer process, not the metal (i.e. magnesium) but the **macrocycle is involved** (cf. in cyt P-450, catalase and peroxidase, the porphyrin ligand is also oxidised by one equivalent; in other metalloproteins, the metal centres participate in the redox processes). This aspect has been discussed in Sec. 8.5.5.

8.5.5 Electron Transport Chain in Light Phase Reactions of Photosynthesis

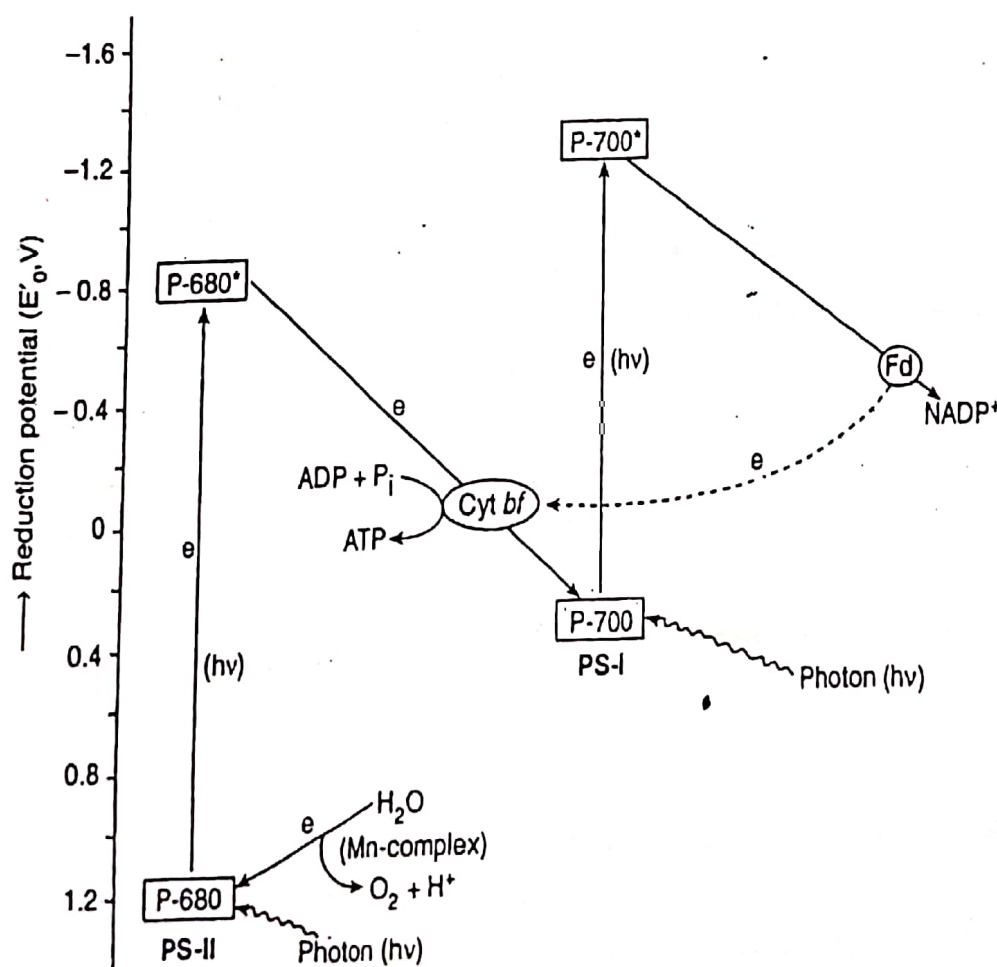
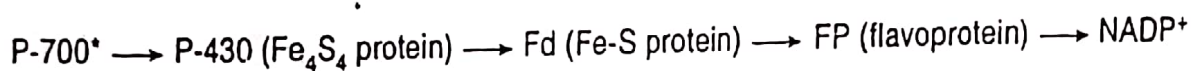
Chlorophyll catalyses the reduction of $NADP^+$ (to NADPH) and oxidation of H_2O (to O_2) in the presence of light. The electron flows from H_2O to $NADP^+$ (without considering the cyclic flow of electrons which will be discussed later) through an electron transport chain (P-680 to P-700*) which looks like Z when the electron carriers are placed in the order of their reduction potentials. Thus the chain is very often described as **Z-scheme**.

The whole process is carried out by two kinds of photosystems. Existence of such two photosystems was established by considering the phenomenon of red drop and the dependence of photosynthetic efficiency on the wavelength of light. This aspect has been already discussed in Sec. 8.5.2. **Photosystem I** (abbreviated as PS-I or P-700, P stands for pigment) which is excited by the light of wavelength in the region 700 nm (or lower) generates a strong reductant to bring about the reduction of $NADP^+$ to NADPH. **Photosystem II** (abbreviated as PS-II or P-680) uses the light of wavelength 680 nm or lower to produce a very strong oxidant to oxidise H_2O to O_2 . PS-I uses chlorophyll- a_1 ($chl-a_1$) while PS-II uses chlorophyll- a_2 ($chl-a_2$). Each photosystem contains ~250 light harvesting pigments (~200 chlorophylls and ~50 carotenoids) in addition to different electron carriers

In terms of the standard reduction potential (under biological conditions, i.e. pH ~ 7.0) of the involved couples, i.e. $\text{O}_2/\text{H}_2\text{O}$ ($E'_0 = 0.82 \text{ V}$) and $\text{NADP}^+/\text{NADPH}$ ($E'_0 = -0.34 \text{ V}$), the electron flow from H_2O to NADP^+ to produce NADPH is a '**thermodynamically uphill**' process. But photoexcitation of PS-I and PS-II can make the electron flow '**downhill**' as shown in the Z-scheme.

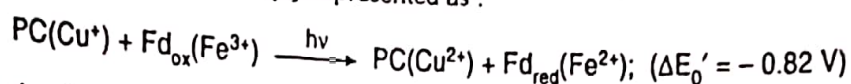
When the chlorophyll (present in PS-I or PS-II) is excited, its electron distribution pattern changes. On excitation, it can act both as a *better reducing agent* (because the excited electrons can be easily removed) and also a *better oxidising agent* (because the positive hole resulted from the excitation of electron can accept electron favourably). Thus the excited chlorophylls can initiate a series of redox reactions.

When P-700 is excited to P-700^* , its reduction potential changes from $+0.4 \text{ V}$ (at the ground state) to about -1.3 V (at the excited state). In fact, the uphill reaction is favoured by the absorption of 700 nm photon ($\equiv 171 \text{ kJ mol}^{-1}$) and the photon energy is utilised to elevate the electron. **Thus P-700^* becomes a better reducing agent** and it transfers its electron to its primary electron acceptor P-430. It is a membrane bound ferredoxin of the Fe_4S_4 type characterised by a strong absorption maxima at 430 nm in the reduced form. Then the electrons flow the downhill and ultimately reach NADP^+ through a series of electron carriers arranged in the increasing order of their reduction potentials. This electron transport chain is shown below.



Scheme 8.5.5.1 : Schematic representation of Z-scheme to represent the electron flow process in light phase reactions of photosynthesis. The dotted route indicates electron flow in cyclic photophosphorylation.

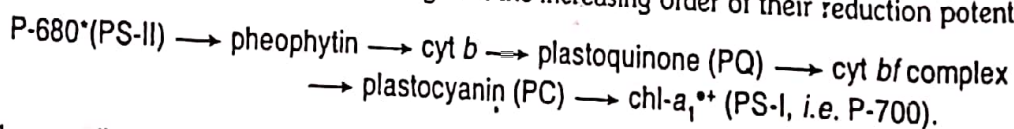
The electron enters into PS-I from plastocyanin (PC), a copper containing blue protein (Sec. 7.3.1). The overall redox reaction catalysed by PS-I involves the electron flow from PC to Fd which subsequently reduces (catalysed by FP, i.e., Fd-NADP reductase) NADP^+ to NADPH. The PS-I catalysed redox reaction can be simply represented as :



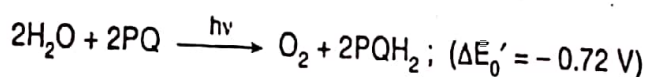
Considering the E_0' values (reduction potentials at biological conditions) + 0.37 V and - 0.45 V for PC and Fd respectively, the standard free energy change ($\Delta G_0'$) for the uphill process is about +79 kJ mol⁻¹. This disfavoured process is driven by the absorption of 700 nm photons ($\approx 171 \text{ kJ mol}^{-1}$).

The flavoprotein (FP) is called *ferredoxin-NADP⁺ reductase*. After transferring an electron from P-700* to P-430, it remains as chl-a₁^{••} (a cation radical). This porphyrin radical is stabilised through its extended conjugation. A similar situation has been observed in the activity of catalase, peroxidase and cyt P-450.

To sustain the process, the oxidised species chl-a₁^{••} in P-700 must be reduced to chl-a₁ so that it may again participate in a catalytic process. The standard reduction potential of O₂/H₂O couple ($E_0' = 0.82 \text{ V}$) is too high to reduce chl-a₁^{••} to chl-a₁ in P-700. To perform the task, PS-II (i.e. P-680) is linked with the PS-I (i.e. P-700). When P-680 is excited to P-680*, the reduction potential changes approximately from + 1.2 V to about - 0.8 V. A 680 nm photon is possessing an energy of 1.82 eV which is utilised to change this reduction potential. **Thus P-680*, acts as a better reducing agent.** In P-680*, the excited chl-a₂[•] transfers its electron to pheophytin (Ph). Then the electrons flow the downhill to reach chl-a₁^{••} (in PS-I). After transferring the electron to pheophytin, chl-a₂^{••} is produced in PS-II. This oxidised species chl-a₂^{••} is then brought to chl-a₂ by water. In this event, O₂ evolution occurs and the process is catalysed by a polynuclear manganese protein called **oxygen evolving complex (OEC)**. The electron transport chain from pheophytin to chl-a₁^{••} is shown below where the electron carriers are arranged in the increasing order of their reduction potential.



The overall reaction catalysed by PS-II is :



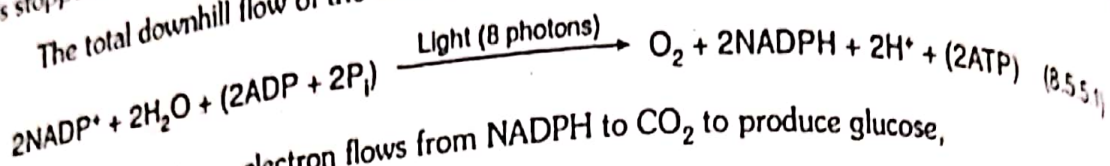
(PQ = Plastoquinone; PQH₂ = Plastoquinol, see Sec. 8.1.1 for structure)

Then the electron reach to plastocyanin (PC) through the cytochrome-bf complex. Considering reduction potentials (E_0') for the PQ/PQH₂ and O₂/H₂O couples as +0.10 V and + 0.82 V respectively, the standard free energy change ($\Delta G_0'$) becomes positive. This uphill reaction is favoured by the absorption of photons of 680 nm ($\approx 176 \text{ kJ mol}^{-1}$) in the PS-II.

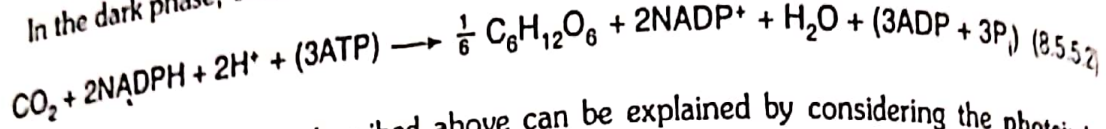
The electron flow pathway from P-680 to P-700* in terms of the redox potential diagram looks like the letter Z and this is why it is very often described as **Z-scheme**.

In the downhill electron flow from P-680* to P-700, ATP is generated. The cytochrome bf complex consists of cyt f (which is a c type cytochrome, f stands for *feuille*, French word meaning leaf), cyt b₅₆₃ (referred to also as cyt b₆), Fe-S protein and a polypeptide chain. This complex is also known as cytochrome b₆f complex. It has been established that during the electron transport via the cytochrome bf complex, the difference of reduction potentials of the involved redox couples is sufficiently high to allow the synthesis of ATP.

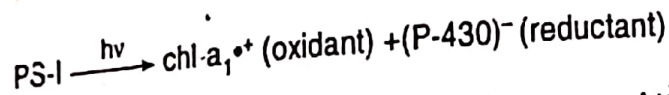
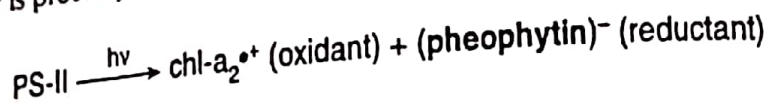
The different herbicides like 3-(3,4-dichlorophenyl)-1,1-dimethylurea (DCMU) can inhibit the electron flow from P-680* to cytochrome *bf* complex and consequently, the photosynthetic activity is stopped. The commonly used herbicides compete with the electron transport agent plastocyanin.



In the dark phase, electron flows from NADPH to CO_2 to produce glucose,

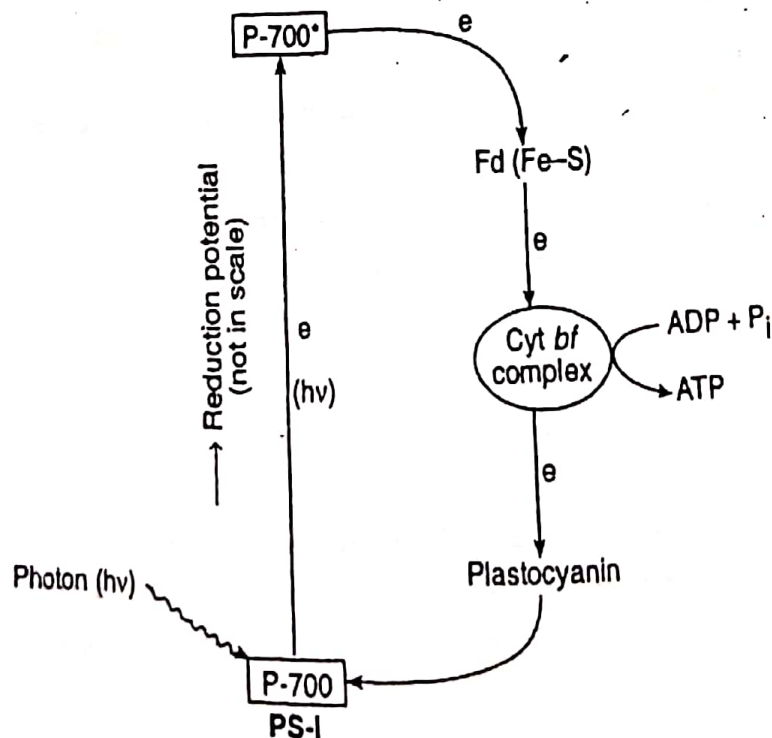


[Note : The Z-scheme described above can be explained by considering the photoinduced charge separation in chlorophyll. The lost electron is captured by a suitable acceptor which then acts as a reductant and the cation radical ($\text{chl}^+\cdot$) acts as an oxidant. In PS-I, the immediate electron acceptor is probably P-430 (bound ferredoxin) while in PS-II it is pheophytin.



In PS-II, $\text{chl-a}_2^+\cdot$ ($E_0' = 1.20 \text{ V}$) is a powerful oxidant and it can oxidize H_2O to O_2 ($E_0' = +0.82 \text{ V}$). In PS-I, the powerful reductant $(\text{P-430})^-$ can reduce NADP^+ to NADPH and $\text{chl-a}_1^+\cdot$ ($E_0' = +0.4 \text{ V}$) can take up the electron from the reductant (pheophytin).]

Cyclic photophosphorylation process in photosynthesis : In the electron transport chain, P-700* to NADP^+ if there is insufficient NADP^+ to accept the electrons from the reduced Fd (via FP), then the high potential electrons flow back to the oxidised form of P-700 through cytochrome *bf*



Scheme 8.5.5.2 : Schematic representation of cyclic flow of electron in PS-I and cyclic photophosphorylation without generation of NADPH.

complex and plastocyanin. It creates a cyclic flow of electrons and during this cyclic flow, ATP is also generated. This is called **cyclic photophosphorylation**.

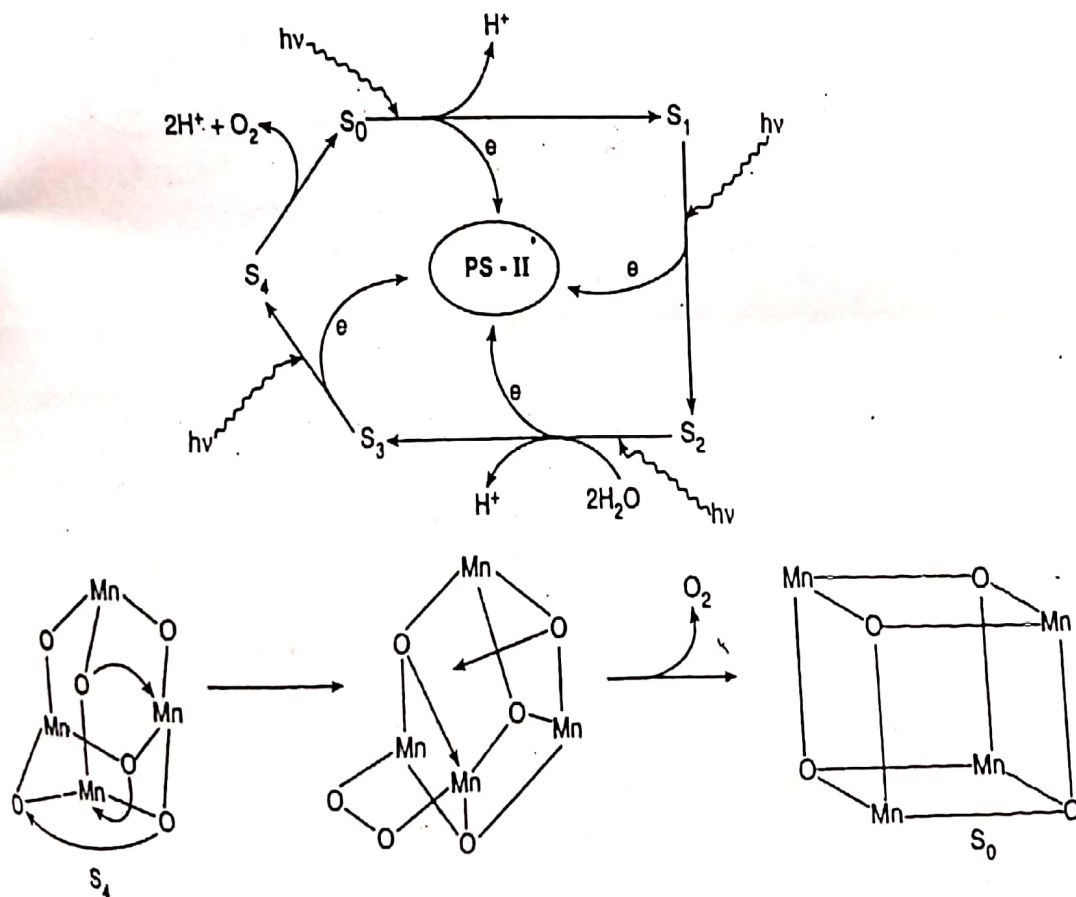
In this cyclic electron flow through PS-I, in fact the high potential electron from P-700* is transported to cyt *b_f* complex rather than to NADP⁺ (Scheme 8.5.5.2). Then this electron flows back to the oxidised form of P-700 via plastocyanin. In this cyclic electron flow, PS-II is not involved and consequently no O₂ is produced from H₂O. However ATP is generated during the electron transfer to plastocyanin via cyt *b_f* complex, but no NADPH is formed.

Water splitting reaction catalysed by Mn-protein in photosynthesis : The oxidised form of PS-II oxidises water and the released electrons enter into the photochemically active centre. The process is catalysed by a **manganese containing enzyme**. The oxidation of H₂O involves the net transfer of 4-electrons.



The P-680* (cation radical) formed in PS-II is a strong oxidant and it extracts electrons from H₂O through the intermediacy of Z factor (i.e. H₂O → Mn-complex → Z → PS-II). It is suggested that the Mn-based enzyme is first oxidised in four one-electron transfer steps and then this oxidised form of the enzyme leads to O₂ evolution. If the Mn(IV)/Mn(II) cycle operates, then the enzyme must contain at least two Mn-centres to accommodate the four-electron transfer process.

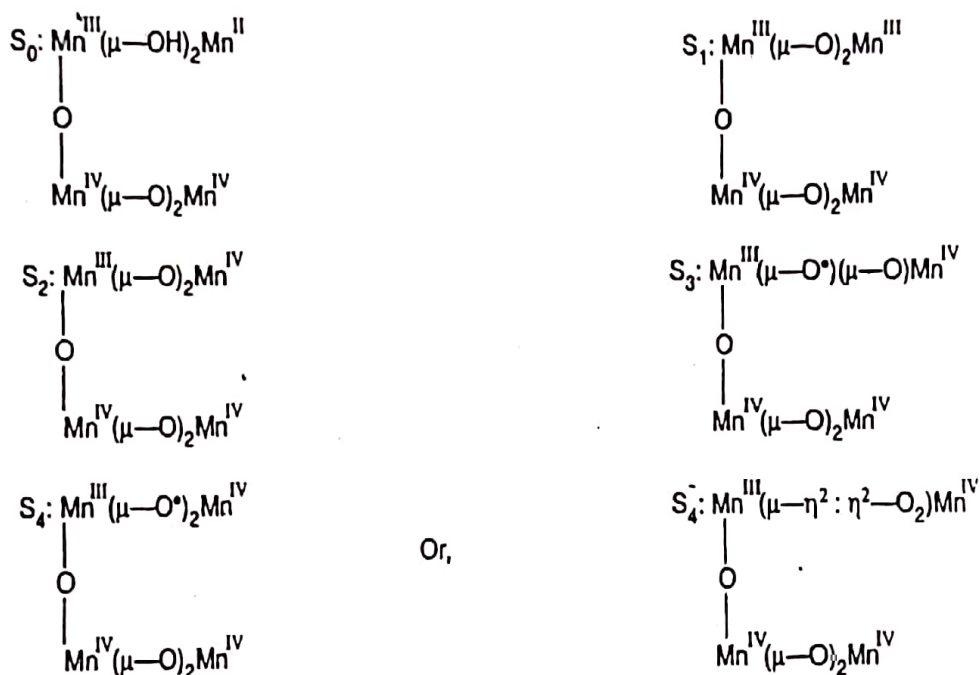
Different models have been proposed to explain the observation. One such popular scheme (known as **Kok cycle**) is discussed below (Scheme 8.5.5.3). The enzyme contains four Mn-centres. This Mn-cluster along with 4-5 Cl⁻ ions and 2-3 Ca²⁺ ions constitute a catalytically active complex known as **oxygen evolving complex (OEC)** which can bind two molecules of water. During extracting of



Scheme 8.5.5.3 : Schematic representation of oxidation of H₂O (i.e. splitting of water) in PS-II catalysed by OEC (oxygen evolving complex, a Mn₄ cluster) in Kok cycle.

electrons from H_2O , protons and O_2 are released. OEC cycles through a series of states designated by S_0, S_1, S_2, S_3 and S_4 . These states are actually the different combinations of Mn(III) and Mn(IV) centres. The OEC is oxidised by P-680⁺ sequentially to different states. The lower states (i.e. S_0, S_1, S_2) are **cubane-like** Mn_4O_4 complexes while the higher states, i.e. S_3 and S_4 , are **adamantane-like** Mn_4O_6 complexes. The sequential electron withdrawal and release of protons and O_2 are shown in Scheme 8.5.5.3. In the conversion of S_4 to S_0 , the adamantane-like structure adopts the cubane-like structure with the release of O_2 . This recovery step (S_4 to S_0) is not light dependent.

The probable oxidation states of Mn in S_0, S_1, S_2, S_3 and S_4 are given in Scheme 8.5.5.4 (other binding sites are not shown).



Scheme 8.5.5.4 : Suggested oxidation states of Mn in different forms S_0, S_1, S_2, S_3 and S_4 in Kok cycle.

It is suggested that for the final step, $S_3 \rightarrow [S_4] \rightarrow S_0$ (where S_4 is probably a transient only), the reduction of a tyrosyl radical occurs with the evolution of O_2 . Here, it is important to mention that Ca^{2+} (which may be replaced by Sr^{2+} to restore the activity) and Cl^- are essential *cofactors* of the Mn-OEC. Their actual role is not yet well established. It is suggested that some bridging ligands (likely carboxylate) bridge the Mn- and Ca-sites and Cl^- acts as '**gate-keeper**' to control the substrate (water) accessibility to tetramanganese core of Kok Cycle. Cl^- may act also as a bridging ligand between the Ca and Mn-centres. Ca-bound water molecule remains hydrogen bonded with the oxo-sites of Mn_4 cluster and this hydrogen bonded water molecule (bound to Ca-site) participates in the activity of the Kok cycle.

There have been several other propositions like **butterfly clusters** (Mn_4O_2) regarding the structure of the Mn-based enzyme.

The reactions occurring in Z-scheme are summarised as :



The electron released in PS-II are transmitted to PS-I as discussed in Z-scheme. Then the dark reaction produces CH_2O by reducing CO_2 with the help of NADPH.

Dark reaction :



Thus the overall reaction is :

